Characterizing and Understanding Self-Assembling, Nanocapsule Host-Guest Systems

---

A Dissertation

Presented to

the Faculty of the Graduate School

University of Missouri ~ Columbia

In Partial Fulfillment

of the Requirements for the Degree

Doctor of Philosophy

By

JENA L. WHETSTINE

Dr. Sheryl A. Tucker, Dissertation Supervisor

MAY 2010

The undersigned, appointed by the dean of the Graduate School, have examined the dissertation entitled

CHARACTERIZING AND UNDERSTANDING SELF-ASSEMBLING, NANOCAPSULE HOST-GUEST SYSTEMS

presented by Jena Whetstine,a candidate for the degree of doctor of philosophy of Chemistry, and hereby certify that, in their opinion, it is worthy of acceptance.

Professor Sheryl Tucker

Professor Elizabeth Giuliano

Professor C. Michael Greenlief

Professor Silvia Jurisson

Professor Jerry Atwood

ACKNOWLEDGMENTS

First, I would like to offer my sincere gratitude to my advisor, Dr. Sheryl Tucker. I could not have asked for a better mentor. She is who I would like to be when I 'grow up'; a strong woman and an awesome chemist. Without her support and the ability to give me a swift kick in the butt when I needed it, I would have never been able to do the things I have accomplished.

I would like to also thank my fellow Tucker groupies, past and present. I cannot picture anyone else better to introduce me to the Tucker group than Dr. Elizabeth Morgan. She is larger than life and leaves a lasting impression. I treasure all the time I spent with her. Thanks to Lisa Norton in expanding my library. I love all the discussions we have and I enjoy talking to a person who likes books as much as I do. To Dr. Katrina Kline, I offer my unwavering loyalty and gratitude. She stuck with me to the end, supporting me and encouraging me along. If she ever needs back-up, I'll be there. And thanks also go to Dr. Joseph Turner and Bill Vellema. These two men have shown me more ways to fix/troubleshoot instrumentation than I could possibly have figured out on my own.

My aunt, uncle and cousin deserve a medal of honor for putting up with me for the last few years. They welcomed me into their home and family with open arms. Cathi will always be the 'Great' aunt my siblings and I adore. Mischief seems to just follow her around. Rob is probably the

oldest child I have ever known, and I absolutely love him for it. Whenever I thought I was taking myself too seriously, I would just spend some time with my Uncle Rob; problem solved. Grant is the other little brother that I did not know I needed. He was always up for watching cartoons, playing a game, or just hanging out. I have been able to watch him grow up and start to discover what type of person he wants to be. I hope I have damaged him too much.

And lastly, I would never be where I am today without my family. I have been blessed with a family that unconditionally loves and supports me. I do not know what I would have accomplished without my mother and father believing in me and being there when I needed them. My siblings have made my life an interesting place to be. I don't know exactly what to say other than crazy works for us. Jess is the strong older sister that we all need to tell us when we are being stupid and encourage us in the right direction. Joanna is the most compassionate cynical person I have ever met. When we are together, nothing can stand in our way, world watch out! Jacob is the little brother; annoying, pestering, and protective all wrapped up in one. What can I say, other than I love him! Bridget, who is new to the family and so far has not run screaming into the night, may be the sanest of the family. She has been a friend that I did not know I needed. Thank you my family for being you.

Characterizing and Understanding Self-Assembling, Nanocapsule Host-Guest Systems

Jena L. Whetstine

Dr. Sheryl A. Tucker, Dissertation Supervisor

ABSTRACT

Supramolecular, self-assembled nanocapsules have been shown to be capable of entrapping fluorescent guests. Previous solid- and solution-state research, focusing on hydrogen-bonded *C*-alkylpyrogallol[4]arenes (PgC_6)nanocapsules, have shed light on the host-guest-relationship potential of these materials. Investigations of these nanocapsules with different fluorophores were undertaken to better understand the guest properties (e.g., size, shape, molecular volume, and functionality) needed to facilitate robust encapsulation. In addition, another relatively new nanocapsule containing metal ions in place of some of the hydrogen bonds was also examined. UV-Visible absorption and steady-state and dynamic fluorescence spectroscopic techniques were used to examine the host-guest interactions between the capsule interior and the fluorescent reporter

molecule pyrene butanol that became encapsulated in the PgC_6 nanocapsule. Solution-state spectroscopic data was compared with solid-state, single-crystal, X-ray crystallographic results. This work supported the hypothesis that the tail functionality of the encapsulated guest is a critical feature for encapsulation and potentially ensures the robustness of that association. The research laid the foundation for understanding how to achieve successful encapsulation of future entities. The work advanced the understanding of the goodness-of-fit criterion between guest and host for these PgC_6 supramolecular, self-assemblies.

TABLE OF CONTENTS

LIST OF TABLES

LIST OF FIGURES

Chapter 1: Introduction

I. Supramolecular chemistry:

Supramolecular chemistry is probably best described by Jean-Marie Lehn in his 1987 Nobel prize work as the 'chemistry of molecular assemblies and of the intermolecular bond',[1] or more simply put by Atwood and Steed 'chemistry beyond the molecule'.[2] One of the more interdisciplinary branches of chemistry, it is perhaps best known for its macromolecular structures and its host-guest chemistry. Like much of science, supramolecular chemistry found its beginnings in nature. Some of the most common supramolecular assemblies are biological in nature: DNA, RNA, and proteins.[3,4] Just recently (i.e., in the last couple of decades) has there been headway made in the development of systems that mimic the functions and properties of the natural biological macromolecular structures.[3,4] Gokel *et.al.* utilized the pyrogallolarenes as pseudo-membranes, testing the ability of the hydrophobic side chains to host various guests.[5] In 1983, Nobel Laureate Aaron Klug spoke about how many biological systems are 'self-assembled, self-organized, and self-checking'.[4] His focus was mainly on the work of Rosalind Franklin,

which focused on the Tobacco Mosaic virus. This particular virus is made of multiple spiraling layers of proteins. Each layer consists of three nucleotides per protein subunit and 16 1/3 subunits per turn of the helix.[6] What made this virus so interesting to Klug was the fact that it self-assembled around an embedded RNA. The formation of hemoglobin from polypeptide subunits utilizes this same principle.[7] Since these processes occur naturally in some biological systems, interest has grown into understanding the concepts and theory behind the self-assembly processes.[8,9]

Supramolecular, self-assembled nanocapsules can be defined as complex macromolecules formed from two or more subunits and held together by some type of intermolecular force; usually van der Waal's interactions, hydrogen bonds, aromatic π-stacking, polar bonds, and more recently metallic interactions.[10] Nanocapsule can be further defined as a general term for a chemical structure capable of hosting a guest in its interior.[2,10] This applies to any molecule or complex that can be found encapsulated by the self-assembled host, up to and including solvent molecules.[11] Rebek *et. al.* experimented with a series of liquid *n*-alkanes (C_5 to C_{20}) that were successfully entrapped in pryogallolarene hexamer.

The presence of encapsulated solvent was determined via ^{1}H NMR and two-dimensional COSY NMR.[11]

Probably the most important feature of self-assembly is that the formation of the self-assembled nanocapsules is not dictated by any specific factor. Two different types of self-assembled nanocapsules are disscussed in this dissertation. The first is a metal-coordinated hexameric nanocapsule made of pyrogallol[4]arene and copper nitrate.[12,13] It is held together with 24 Cu(II) metal ions and 48 hydrogen bonds (H-bonds).[12,13] The second nanocapsule is composed of six pyrogallol[4]arenes and is held together with 72 H-bonds.[3-4,8-10,14-15]

Supramolecular self-assembled nanocapsules have a multitude of potential applications. For instance, they would make useful models for complex biological processes.[8,9] They also are able to shed light on the interesting concept that is 'lock and key' chemistry. Paul Enhrlich is probably one of the first to be intrigued by this concept and use it when studying infectious dieases.[2] Another biological system that supramolecular, host-guest chemistry hopes to illuminate is the cell. Cells are naturally occurring 'hosts' to many different 'guests' inside a protected environment. Understanding the interactions between a host and its guest, tracking the changes of the interior microenvironment, and

investigating the properties of the guest that affect the mircoenvironment would be a huge advancement in understanding and mimicking cell behavior. Scientists are currently working on how to probe and monitor the inner workings of cells without destroying them.[16]

Another current supramolecular chemisty reserach focus is the possiblity of using nanocapsules in drug delivery.[17] Most doctors prefer to prescribe as little medication as possilble; one pill weekly vs. one pill daily.[18] Ultimately, it is hoped that a nanocapsule could be produced that could carry the drug of choice to the damaged or affected site in the human body, slowly release the medication over time, and then be discarded through natural bodily processes. This then would use less drug, leading to overall decrease in cost, decrease in the number of pills taken, decrease in side effects, and hopefully a decrease in recovery time or an increase in recovery rate.

A more chemical application of nanocapsules is the use of Sephadex® in separations. Sephadex® is a macromolecule that ultizes small hydrophobic pockets to trap smaller molecules allowing large molecules to elute off of a column first. Recently, it was successfully used for clean fullerene separation.[19]

II. A Short History of Synthesized Self-Assembled Nanocapsules:

Supramolecular chemistry can trace its origins back to the earliest of chemistries, but only within the last few decades has the potential of this branch of chemistry been exploited. In 1989, one of the early capsules, a carceplexe, was made by Cram *et al.* and was held together by covalent bonds.[21] Almost a decade later, a non-covalent, self-assembled nanocapsule was synthesized,[10] and in 1997 Atwood *et al.* synthesized a 'snub-nosed cube' which was relatively larger than the previous capsule. It had an interior volume of 1500 $Å^3$ and was held together by 60 H-bonds.[9] Three years later Mattay *et al.* used pyrogallol as a subunit instead of resorcinol and synthesized a similar nanocapsule that was held together by 72 H-bonds (Figure 1.1).[20]

The difference between pyrogallol and resorcinol is one hydroxyl group. Resorcinol has two *meta*-hydroxyl groups while pyrogallol has three *ortho*-hydroxyl groups. The extra hydroxyl group gave the capsule more strength than the 'snub-nose cube' since there are a total of 72 H-bonds versus 60. This nanocapsule is stable in polar solvents, and the R-groups can vary from a carbon chain to any number of ligand groups. By

manipulating the size of the R-group, the hydrophobicity can be changed.

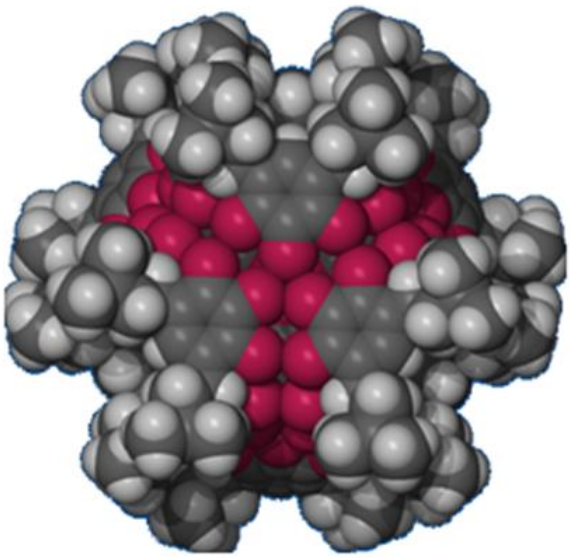

Figure 1.1 Pyrgallol[4]arene nanocapsule that contains 72 H-bonds, 12 from each macrocycle, which are indicated by the red. This figure is reproduced from Atwood *et al.* 2002.

The interior volume of this nanocapsule is ~1200 Å^3, and therefore, smaller molecules can be contained within it. This particular nanocapsule has been utilized as a host for a few different fluorophores as guests.[3-4,21] In particular, the solid- and solution-state properties were examined with pyrene butyric acid as a guest.[4] Although this nanocapsule has been thoroughly examined through solid-state means

and headway has been made into the host-guest interactions in the solution state, much is still not known. The pyrogallol building-block nanocapsule is one that this dissertation examines in the hopes of characterizing and understanding the host-guest interactions and relationships, via solution-state investigations.

In 2005, Atwood *et al.* produced a new nanocapsule that was similar in structure to the previously discussed hexameric nanocapsule, with the exception that it contains copper metal ions in the place of some of the H-bonds (Figure 1.2).[12]

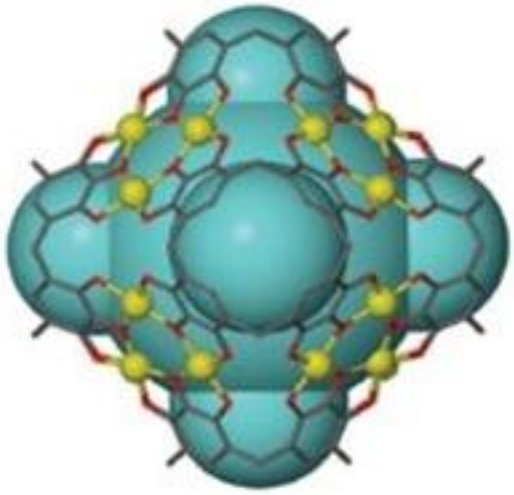

Figure 1.2 A metal-containing nanocapsule formed by combining pyrogallol[4]arene with copper(II) nitrate. There are 96 Cu-O bonds (yellow and red) and 24 hydrogen bonds (not shown). The figure reproduced from McKinlay *et al.* 2005.

While hexamers have been of interest in the past, these new supramolecular assemblies were able to form dimers, tetramers, and hexamers by varying temperature and controlling the amount of water introduced to the system.[22] These relatively new nanocapsules are more robust and have a much greater stability than their counterparts with only H-bonds. The metal-containing macromolecules assemble more rapidly than their hydrogen bound analogs and readily exchange their H-bonds for metal ions.[23]

Along with the copper nanocapsule, gallium, cesium, and zinc have been successfully used as metal seams. The cesium and zinc nanocapsules have been found to form dimers, with eight metal ions, while the gallium forms a hexameric "rugby-ball", which contains 12 Ga(III) atoms.[13] Most recently, there has been investigation into Ga/Cu and Ga/Zn coordinated nanocapsules.[21] However, as with any of these supramolecular assemblies, solid-state data is readily available and has been thoroughly examined, but the solution-state investigations are still uncharted territory.

In a more physical application, a Purdue University research group designed and tested a "nano-ring" with several cobalt atoms self-assembled under a magnetic field.[24] This ring was first introduced to

speed computer memories and enhance the data storage capabilities.[25] These are just a few of the more prominent applications for supramolecular nanotechnology. Investigations into host-guest chemistry will not only aid chemists, but researchers in other areas of chemical, material, and biological sciences.

The host-guest properties of the metal-containing nanocapsules are not well understood. The ability of the copper-containing capsules to contain a guest other than solvent, whether in solid or in solution is unknown. Needless to say, this is the second nanocapsule this dissertation will examine. Similar criteria that govern the host-guest association in the aforementioned hydrogen-bonded nanocapsules, are also of consideration with copper-containing species:

- Formation requires enough tetramers are available for encapsulation.
- Guest molecule should not interfere with the self-assembly of the macrocycle.
- Capsule has to be in a solvent that does not affect its stability, while still encouraging guest occupation.
- Guest molecules must be smaller than the interior volume of the capsule.

Once the capsules have formed, an examination into how the interior is organized, via solid and/or solution state, is needed. The majority of studies into any supramolecular assembly are normally focused on solid-state data and organization. However, this is problematic when many desirable applications for this branch of chemistry take place in solution. This is where the collaboration between the Atwood and Tucker Research Groups is highly beneficial. Fluorescence spectroscopy, with its high sensitivity and selectivity, can be utilized in the solution state to determine guest occupation. This approach is used to provide valuable information about these materials and is the expertise of the Tucker Group.

III. The Fluorescence Spectroscopy Approach:

The use of fluorescent reporter molecules to examine these unique self-assembled systems is still relatively new and was pioneered in the Tucker Research Group. While our earlier work and the research presented here concentrates on entrapping a fluorescent guest, work by Rebek *et.al.* has successfully attached two different fluorescent guests to the exterior of the same hexamer.[26] Using a combination of fluorescence

resonance energy transfer (FRET) and ^{1}H NMR, the hexamers with two different fluorophores attached could be deciphered from the hexamers that only contained multiples dye molecules of the same fluorophore.[26] This work utilizes a broader array of steady-state and dynamic fluorescence spectroscopic measurements, including traditional quenching.

Fluorescence spectroscopic techniques are a well-documented way to study complex systems. Because of the sensitivity, they can be used to trace small amounts of fluorophores (10^{-9} M) in complex environments. Moreover, due to minimal sample perturbation, these measurements can be used in monitoring self-assembly processes, where other guest molecules might interfere with the production of the desired product. Because of the multiple dimensions, fluorescence is also highly selective, and experiments can be tailored to fit a particular system as needed.

So-called "fluorescent probes" can be used to monitor and report information about the local environment. These reporter molecules are widely used in both chemical and biological systems.[27-34] Fluorescent probes respond to different aspects of the surrounding microenvironment, resulting in predictable patterns that can be observed in the fluorescence signals. Some of these environmental factors are

illustrated in Figure 1.3. Changes to the fluorescence signal can manifest as fluctuations in emission intensity (increase or decrease), spectral wavelength shifts (red or blue), differences in the fluorescence lifetimes (longer/shorter or the appearance of a completely new lifetime component), or the disappearance/appearance of excitation/emission peak(s) in a fluorescence fingerprint.[35] Once a probe (guest) is successfully placed in a particular system, incredible information can then be extracted thorough a series of well-planned experiments.

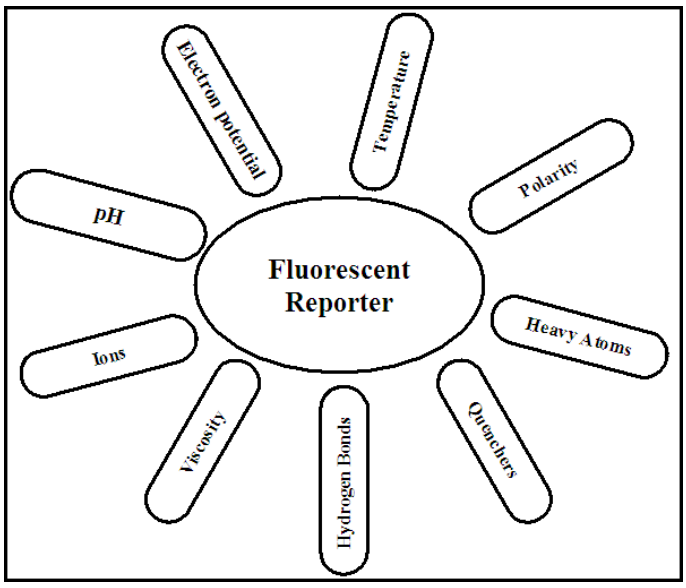

Figure 1.3 Diagram showing the different environmental factors that can affect fluorescent reporters. (Diagram reproduced from Bernard Valeur 1993)[36]

Possible information obtained can be as simple as probe location to the more difficult to determine, like microenvironmental conditions such as polarity and hydrophobicity, area openness, and structural rigidity. Using a fluorescent reporter molecule to its full potential is beneficial in investigating the aforementioned host-guest chemistry.

IV. Probing Nanocapsules with Fluorescent Reporter Molecules:

As mentioned previously, the two self-assembling nanocapsules studied here are complex supramolecular systems that have been studied in the solid state.[3-6,10-14,21-23] However, investigations into the host-guest properties of copper pyrogallol[4]arene ($CuPgC_n$) and the hydrogen bonded pyrogallol[4]arene (PgC_n) are incomplete at best, particularly solution-state studies. Previous work into the PgC_6 nanocapsule revealed that guest conformational flexibility and functional-group chemistry play a role in the ease with which encapsulation occurs. To determine how these parameters affect guest encapsulation, a series of polycyclic aromatic hydrocarbons (PAHs) were utilized. Traditionally, PAHs are common probes of complex systems.

They are highly fluorescent and have many different structures differing in the number of aromatic rings and in functional groups.[37]

In this work, several PAHs, mainly pyrene derivatives, were used to further investigate the PgC_n nanocapsule. The pyrene derivatives all had the original parent fluorescent moiety, differing only in functional group attached. By using the same fluorescent moeity, trends between guest encapsulation and the functionality of the probe could be monitored. The pyrene derivatives are also used to examine the 'tail' length significance on encapsulation by keeping functionality constant and changing the length of the carbon chain.

A slightly different approach was taken with the $CuPgC_n$ nanocapsule, since no previous work had been done on the system. External attachment to a copper ion, as well as encapsulation (internal) of a probe molecule, was investigated. The PAHs were again utilized, as well as other types of fluorescent dyes with the appropriate functionality, in order to facilitate the host-guest chemistry of this supramolecular system of interest.

Characterization of these two different nanocapsules in solution is discussed within this dissertation. Efforts were focused on attachment or encapsulation of a probe for the $CuPgC_n$ nanocapsule and narrowing the

parameters for guest selection for the PgC_n nanocapsule. Previous work by the Tucker Research Group has successfully studied encapsulated pyrene butyric acid and 1-(9-anthryl)-3-(4-dimethylaniline)propane in the PgC_6 nanocapsule. The solution-state studies found that, when dissolved, the probe of interest was still encapsulated by the PgC_6 nanocapsule along with solvent molecules of assembly. These unique systems showed interactions between the capsule walls and the probe molecule itself while in solution. It was hypothesized that the probe linker or 'tail' functionality could aid in the encapsulation process. The 'tail' functionality of various fluorescent probes and host-guest complex stability after encapsulation in the PgC_6 nanocapsule will be investigated.

V. References:

(1) Lehn, J. M. *Supramolecular Chemistry: Concepts and Perspectives*, 1995.

(2) Atwood, J. L.; Steed, J. W. *Supramolecular Chemistry*. John Wiley & Sons, Ltd: New York, 2005; p. 745.

(3) Dalgarno, S. J.; Bassil, D. B.; Tucker, S. A.; Atwood, J. L. *Angew. Chem., Int. Ed.* **2006**, *45*, 7019-7022.

(4) Dalgarno, S. J.; Tucker, S. A.; Bassil, D. B.; Atwood, J. L. *Science* **2005**, *309*, 2037-2039.

(5) Kulikov, O. V.; Rath, N. P.; Zhou, D.; Carasel, I. A.; Fokel, G. W. *New J. Chem.* **2009**, *33*, 1563-1569.

(6) Klug, A. *Angew. Chem.* **1983**, *95*, 579-96.

(7) Ackers, G. K. *Biophys. J.* **1980**, *32*, 331-46.

(8) Cave, G. W. V.; Antesberger, J.; Barbour, L. J.; McKinlay, R. M.; Atwood, J. L. *Angew. Chem. Int. Ed.* **2004**, *43*, 5263-5266.

(9) MacGillivray, L. R.; Atwood, J. L. *Nature* **1997**, *389*, 469-472.

(10) Conn, M. M.; Rebek, J., Jr. *Chem. Rev.* **1997**, *97*, 1647-1668.

(11) Palmer, L. C.; Rebek, J., Jr. *Org. Lett.* **2005**, *7*, 787-789.

(12) McKinlay, R. M.; Cave, G. W. V.; Atwood, J. L. *PNAS* **2005**, *102*, 5944-5948.

(13) Dalgarno, S. J.; Power, N. P.; Atwood, J. L. *Coord. Chem. Rev.* **2008**, *252*, 825-841.

(14) Whetstine, J. L.; Kline, K. K.; Ragan, C. M.; Barnes, C; Atwood, J. L.; Tucker, S. A. S*pectroscopic Investigations of*

Pyrene Butanol Encapsulated in C-hexylpyrogallol[4]arene Nanocapsules. unpublished work.

(15) Bassil, D. B. Ph.D. Dissertation, University of Missouri-Columbia, **2007**.

(16) Zandonella, C. *Nature* **2003**, *423*, 10-12.

(17) Shi, X.; Wang, S.; Chen, X.; Meshinchi, S.; Baker, J. R., Jr. *Mol. Pharm.* **2006**, *3*, 144-151.

(18) Chen, B. H.; Lee, D. J. *J. Pharm. Sci.* **2001**, *90*, 1478-1496.

(19) Atwood, J. L.; Koutsantonis, G. A.; Raston, C. L. *Nature* **1994**, *368*, 229-31.

(20) Gerkensmeier, T.; Iwanek, W.; Agena, C.; Frohlich, R.; Kotila, S.; Nather, C.; Mattay, J. *Eur. J. Org. Chem.* **1999**, 2257-2262.

(21) Dalgarno, S. J.; Szabo, T.; Siavosh-Haghighi, A.; Deakyne, C. A.; Adams, J. E.; Atwood, J. L. *Chem. Comm.* **2009**, 4339-1341.

(22) Mossine, A. V.; Atwood, J. L. *Abstract*, 44th Midwest Regional Meeting of the American Chemical Society, Iowa City, IA, United States, October 21-24 2009.

(23) Jin, P.; Dalgarno, S. J.; Warren, J. E.; Teat, S. J.; Atwood, J. L. *Chem. Comm.* **2009**, 3348-3350.

(24) Tripp, S. L.; Dunin-Borkowski, R. E.; Wei, A. *Angew. Chem., Int. Ed.* **2003**, *42*, 5591-5593.

(25) Sherman, J. C.; Cram, D. J. *J. Am. Chem. Soc.* **1989**, *111*, 4527-8.

(26) Barrett, E. S.; Dale, T. J.; Rebek, J., Jr. *Chem. Commun.* **2007**, 4224-4226.

(27) Katusin-Razem, B.; Wong, M.; Thomas, J. K. *J. Am. Chem. Soc.* **1978**, *100*, 1679-86.

(28) Reichardt, C. *Chem. Rev.* **1994**, *94*, 2319-2358.

(29) Ribou, A.-C.; Vigo, J.; Salmon, J.-M. *Photochem. Photobio.* **2004**, *80*, 274-280.

(30) Richter-Egger, D. L.; Landry, J. C.; Tesfai, A.; Tucker, S. A. *J. Phys. Chem. A* **2001**, *105*, 6826-6833.

(31) Richter-Egger, D. L.; Tesfai, A.; Tucker, S. A. *Anal. Chem.* **2001**, *73*, 5743-5751.

(32) Morgan, E. J.; Rippey, J. M.; Tucker, S. A. *Applied Spect.* **2006**, *60*, 551-559.

(33) Kline, K. K.; Tucker, S. A. *J. Phys. Chem.* **2009**, *113*, 12891-12897.

(34) Kline, K. K.; Morgan, E. J.; Norton, L. K.; Tucker, S. A. *Talanta* **2009**, *78*, 1489-1491.

(35) Lakowicz, J. R. *Principles of Fluorescence Spectroscopy*; Plenum Press: New York, 1983.

(36) Valeur, B. *Molecular Luminescence Spectroscopy* **1993**, *77*, 25-84.

(37) Tucker, S. A. Ph.D. Dissertation, University of North Texas, **1994**.

Chapter 2: Theory

The research project described in this dissertation involves investigating two different types of nanocapsules with fluorescent reporter molecules and understanding the nature of the host-guest complexes. This work is a collaboration between the Atwood and Tucker research groups. The work described here focuses on the solution-state work performed using traditional molecular spectroscopy tools: UV-Vis absorption and fluorescence emission and lifetime measurements. These experiments were carried out in conjunction with solid-state experiments, primarily single-crystal, X-ray diffraction methods, contributed by the Atwood Research Group. Comparisons focus on the solid- and solution-state behavior.

I. Absorption Spectroscopy:

When beginning the solution-state work on the respective supramolecular assemblies, the first measurement taken is an absorption spectrum. This process is useful in determining where the system of interest absorbs, revealing any ground-state interactions

between the analytes in the system, and potentially the concentration of the absorbing analytes.

This measurement is usually taken by scanning a wavelength region of interest. The resulting data is presented as a spectrum of absorbance intensities in AU (absorbance units) versus wavelength in nanometers of the scanned region. It should be noted here that absorption is a process by which light is absorbed. Absorbance is the quantification of that light absorbed, i.e., a numerical value.

The mathematical relationship describing molecular absorption was first noted by August Beer in 1852, Johann Heinrich Lambert in 1760, and Pierre Bouguer in 1729; it is known as Beer-Lambert-Bouguer law or more commonly Beer's Law (Equation 2.1 and 2.2):

$$A = \varepsilon bc \qquad \textbf{Equation 2.1}$$

$$A = -\log T = \frac{I}{I_0} \qquad \textbf{Equation 2.2}$$

where 'A' is the absorbance, 'ε' is the molar absorptivity in L mol^{-1} cm^{-1}, which is the amount of light absorbed by one molar concentration of the species present and can be determined by measuring the absorbance of a known concentration: 'T' is the transmittance; 'b' represents the

pathlength or the sample container size in cm (typically 1 cm); and 'c' is the concentration of the molecule in mol L^{-1}. Molar absorptivities are larger than 10,000 for highly absorbing molecules and much smaller for weakly absorbing molecules.[2] Transmittance, commonly given as percent transmittance %T, is a quantity that reflects the amount of light passing through the solution compared to the reference signal (I/I_0). Since transmittance and absorption are inversely related, when a species has a high absorbance, that same species is transmitting less or has a lower percent transmittance. For the research presented in this body of work, the pathlength was constant at 1.0 cm. This in turn, allows for an easy quantification, since absorbance is directly proportional to the concentration of the analytes in the system of interest. However, there are a few factors that can affect this linear relationship between concentration and absorbance.[1,2] One such factor is an absorbance intensity exceeding 1 AU, due to high solution concentrations. For the linear relationship to be optimal and for a quantitative measurement the absorbance should be below 0.1 AU.

II. Fluorescence Spectroscopy General Theory:

Figure 2.1 represents a modified Jabłoński energy diagram showing the fluorescence emission path of one molecule after its absorption of light of the appropriate energy. Ground (S_0) and excited (S_1 or S_2) electronic states, vibrational levels (ν_n), absorption (A), fluorescence emission (B), vibrational relaxation (C), and internal and external conversion (D, E) are noted. The energy difference (Equation 2.3) between S_1 and S_0 is proportional to the frequency (υ) of light or inversely proportional to the wavelength (Equation 2.4):[1,2]

$$E = h\nu \qquad \textbf{Equation 2.3}$$

$$E = \frac{hc}{\lambda} \qquad \textbf{Equation 2.4}$$

where h is Plank's constant (6.626 x 10^{-34} J.s), c is the speed of light (2.998 x 10^{8} m.s^{-1}), λ is the wavelength in meters and υ is the frequency in Hertz (s^{-1}).

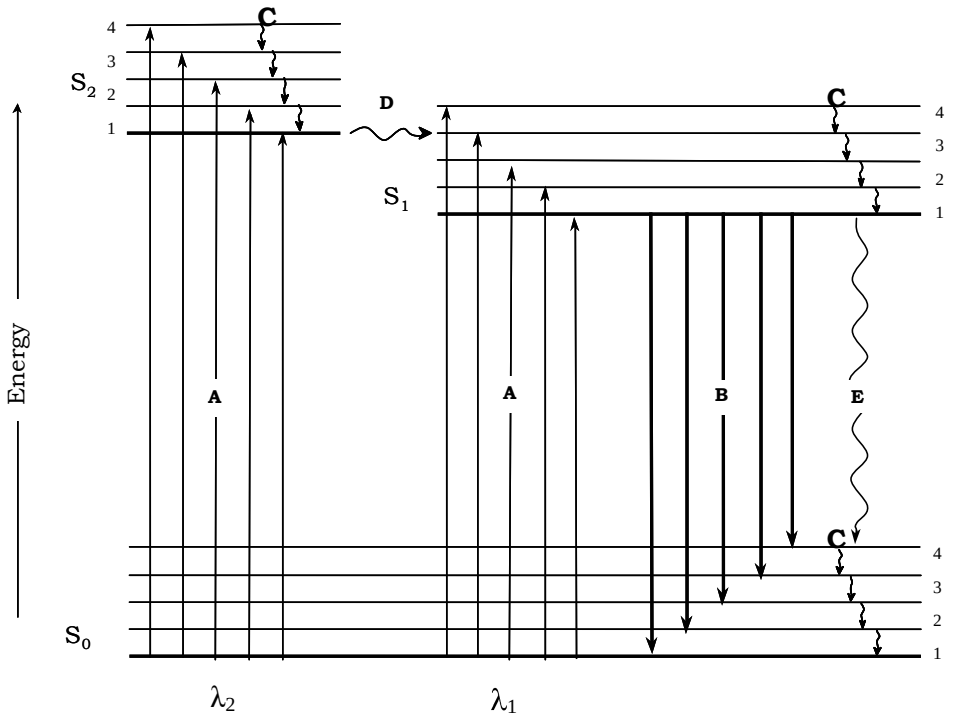

Figure 2.1 Modified Jabłoński diagram showing the events that may occur post absorption/excitation. Ground (S_0) and excited (S_1 or S_2) electronic states, (ν_n) vibrational levels, absorption (A), fluorescence emission (B), vibrational relaxation (C), and internal and external conversion (D, E). Solid lines are indicative of radiative processes and wavy lines represent non-radiative pathways. (Redrawn from *the Principles of Fluorescence Spectroscopy*[3]).

After absorption (~10^{-15} s) takes place,[1] vibrational relaxation occurs permitting the relaxation of electrons to the lowest vibrational level in the excited state. The average vibrational relaxation time is on the order of 10^{-12} seconds.[1]

Fluorescence spectroscopy is the main technique used in the research presented here. Detection limits are typically *ca.* 10^{-10} mol L^{-1} versus commonly used techniques, such as ^{1}H-NMR, which require significantly higher concentrations.

The rate of fluorescence emission (k_{fl}) is measured as an excited state molecule in the lowest vibrational level of the first excited state (S_1, Figure 2.1) returns to the ground state (S_0). There are three main mechanisms that compete with fluorescence emission: intersystem crossing (k_i; 10^{-12} – 10^{-4} seconds), which may result in phosphorescence (10^{-12} - 10^{2} seconds), internal conversion (k_{ic}; 10^{-12} seconds), and external conversion (k_{ec}).

All of the mechanisms mentioned above are radiationless, aside from phosphorescence. Fluorescence emission may occur from 10^{-9} to 10^{-6} seconds, where molecules minimize the amount of time they spend in the excited state.[1,2,4]

The fluorescence emission spectrum (emission wavelength is plotted against the relative fluorescence intensity) is normally independent from the excitation wavelength. Excitation and absorbance spectra for fluorescent species in a solution may be the same if, and only if, all molecules that absorb also emit. The amount of fluorescence

emission can be quantitated and expressed as quantum yield (Φ_{fl}, Equation 2.5):

$$\Phi_{fl} = \frac{k_{fl}}{(k_{fl} + k_i + k_{ic} + k_{ec})} \qquad \textbf{Equation 2.5}$$

The quantum yield is the ratio of the radiative relaxation rate over the total radiative and nonradiative rates.

A more general overview is:

$$k_{nr} = k_{fl} + k_i + k_{ic} + k_{ec} + k_{rxn} + k_q \qquad \textbf{Equation 2.6}$$

where k_{nr} is the rate of the nonradiative relaxation, k_{rxn} is the rate calculated from an intramolecular reaction and k_q is the rate due to the fluorescence quenching, such as from oxygen present in solution. The intensity of the fluorescence (I_{fl}) is proportional to the quantum yield and the number of absorbed photons (Equation 2.7):

$$I_{fl} = k(\Phi_{fl})P_0(1\text{-}10^{-\varepsilon bc}) \qquad \textbf{Equation 2.7}$$

when at low concentrations (c << 0.05 mol L^{-1} most preferably when absorbance is approximately 0.01). The fluorescence intensity is proportional to the absorbance (Equation 2.8):

$$I_{fl} = k(\Phi_{fl})P_0\varepsilon bc \qquad \textbf{Equation 2.8}$$

where k is the instrument constant, and P_0 is the excitation intensity. At low concentrations fluorescence is a more selective and more sensitive technique than absorption, since the relationship between the fluorescence emission intensity is linear with the concentration while absorbance *vs.* the concentration has an exponential relation (Equation 2.9):

$$I = I_0 e^{-\varepsilon bc} \qquad \textbf{Equation 2.9}$$

Fluorescence emission and excitation scanning are commonly used techniques. With fluorescence emission scans, the excitation wavelength is fixed and the emission monochromator is scanned, resulting in an emission spectrum. Excitation scanning is the opposite, where the emission wavelength is set and the excitation monochromator is scanned. When both the emission and excitation wavelengths are

scanned sequentially, the technique is called synchronous scanning and can be used to produce an excitation-emission matrix (EEM). Such a three-dimensional fingerprint gives a more in-depth idea of the different emitting species present in solution.

III. Dynamic Fluorescence Spectroscopy:

III.a. Fluorescence Lifetimes:

The average time a fluorescent molecule stays in the excited state before it decays to the ground state is known as the fluorescence lifetime. Contrary to fluorescence emission intensity values that are in arbitrary units, the lifetime values measured are absolute units. Depending on the environment present, fluorescent reporters may have different lifetimes. Factors that can affect the lifetime are temperature, pH, polarity, viscosity, and oxygen. Just like other fluorescence techniques, the lifetime measurement is sensitive and can provide additional information about the system of interest and the probe environment in solution. For example, once the guest (probe) is encapsulated within the host (PgC_6), it is contained within a protected environment which will make the lifetime

longer. Dendrimers, macrocycles, or even viscous solvents are examples of protected environments that lessen the impact from collision deactivation.[1] Unlike steady-state emission measurements that are an overall average, lifetime measurements reveal true time complexity of the sample under investigation.

Fluorescence lifetimes in this study were measured in the frequency domain, which uses a sinusoidally modulated light source, typically a continuous wave (CW) laser, to excite the fluorophore. The resulting emission is accordingly sinusoidal and modulated at the same circular frequency (ω). The circular frequency is equal to $2\pi f$, where f is the applied linear frequency. The fluorescence emission that has the same frequency will be delayed with a phase shift and the signal will be reduced (demodulated) as shown in Figure 2.2.[1,3,5]

The phase (τ_p; Equation 2.10) and the modulation (τ_m; Equation 2.11) lifetimes are calculated respectively from the phase shift (φ_ω) and the demodulation factor (m_ω):[1,3,5,6]

$$\tau_p = \frac{(\tan\varphi_\omega)}{\omega} \qquad \textbf{Equation 2.10}$$

$$\tau_m = \frac{[\frac{1}{(m_\omega)^2} - 1]^{1/2}}{\omega} \qquad \textbf{Equation 2.11}$$

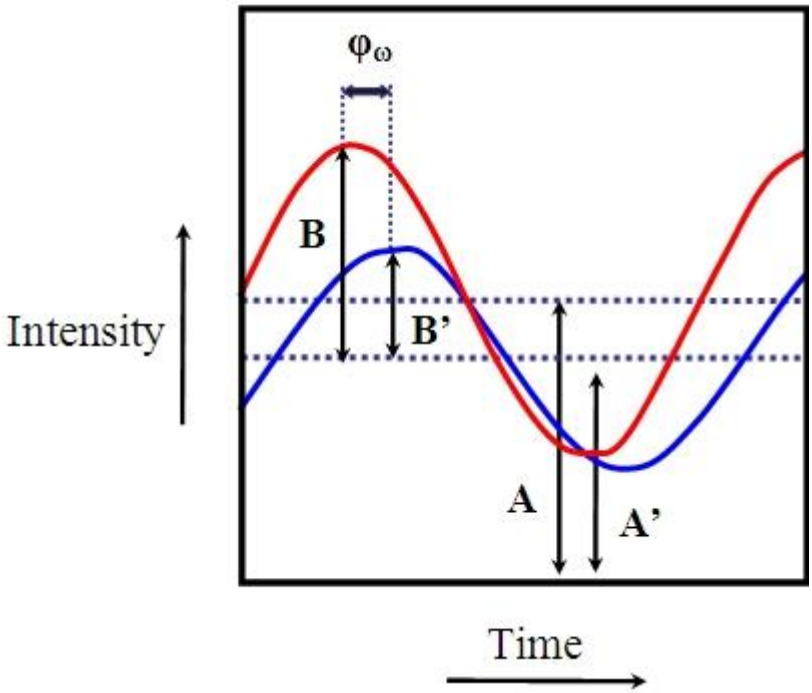

Figure 2.2 Modified phase and modulation diagram for the excitation of a reporter with the modulated light source, where φ_ω is the phase shift between the excitation (red) and the emission (blue) signals.[1] The dynamic to steady state intensity for the excitation and emission are respectively the ratios of B/A and B'/A', where A and A' represent the steady-state intensity, B and B' represent the dynamic-state intensity.

The demodulation factor can be thought of as a ratio of the dynamic-state intensity (B or B') to steady-state intensity (A or A') for both excitation and emission signals (Equation 2.12):[7]

$$m_\omega = \frac{\text{Emission Intensity}}{\text{Excitation Intensity}} = \frac{A \times B'}{A' \times B}$$ **Equation 2.12**

In this technique, the fluorescence lifetime is inversely proportional to the linear applied frequency according to both Equations 2.10 and 2.11. For a single exponential decay, both the phase and modulation can be used to determine the actual lifetime of the fluorophore. For instance, a modulation frequency of 50 MHz and a lifetime of 8 ns, the phase angle calculated from Equation 2.10 would be 68.3°, and the modulation factor calculated from Equation 2.11 would be 0.37, where ω is 2π x 50 MHz. The lifetime and the demodulation factor have an inverse relationship, but the lifetime and the phase angle have a linear relationship.[1,3]

The frequency-domain, fluorescence lifetime instrument used in the course of this research utilizes a multi-harmonic frequency (multi-harmonic Fourier transform) modulator, where a synthesizer provides a base frequency and 60 harmonics are generated by a harmonic modulator. This technique allows for the simultaneous collection of both φ_ω and m_ω values across a range of frequencies that correspond to typical fluorophore lifetime values. The multi-harmonic Fourier transform, MHF, technique is advantageous over others, since it provides a wide range of generated frequencies to cover a "lifetime window".[8,9] Frequency-domain

methods that do not utilize MHF technology consist of taking individual measurements over several frequencies to determine the correct lifetime of the species present in solution.[1] For complex chemical systems, MHF works better since the several lifetimes that may be present in the sample are accounted for by the windowing. The process is fairly fast since the measurement of φ_ω and m_ω are taken simultaneously at all frequencies, a data set of sample and reference pairs can be collected in about 7 seconds with 50 internal averages. Before sample measurements are collected, a scatter solution is used as a calibration marker to accurately determine the lifetime of the reference used. The scatter used in this study was Kaolin where $\varphi_\omega = 0$ and $m_\omega = 1$.

III.b. Lifetime Data Analysis:

Lifetime data was analyzed by the non-linear least square (NLLS) SLM computer software provided by the manufacturer. In NLLS analysis, the goodness-of-fit parameter (χ^2; Equation 2.13) is minimized to determine whether the model is appropriate for the data. Non-linear least square analysis is widely applied for monoexponential species (Equation 2.14) and for multiexponential (Equation 2.15), where F_0 is the initial

intensity, α_i the pre-exponential factor, and τ represents the decay of the fluorophore.

$$\chi^2 = \sum_{\omega} \left(\frac{(\varphi_{\omega,calc} - \varphi_{\omega,obs})^2}{\sigma_{\omega,\varphi 2}} + \frac{(m_{\omega,calc} - m_{\omega,obs})^2}{\sigma_{\omega,m2}} \right) / (N - M - 1) \quad \textbf{Equation 2.13}$$

$$F(t) = F_0 e^{-t/\tau} \quad \textbf{Equation 2.14}$$

$$F(t) = \sum_i \alpha_i F_0 e^{-t/\tau} \quad \textbf{Equation 2.15}$$

By using NLLS analysis (Equation 2.13), lifetimes and fractional intensities are resolved, where $(\omega, calc)$ and (ω, obs) correspond to the calculated and observed values of the circular frequency (ω), respectively. The standard deviation between the calculated and observed ($\sigma_{\omega,\varphi}$ and $\sigma_{\omega,m}$) for the phase and the modulation are determined at a specific frequency, respectively. The total number of data, N, is twice the number of frequencies since both (φ) and (m) are measured at each frequency. The number of unknown lifetimes and fractional intensities is represented by the variable M. The x^2 is considered statistically valid if its value is between one and two.[11,12] The NLLS method is desirable when

working with a well-behaved sample, such that the fluorescent component signatures are known.[8]

IV. Fluorescence Quenching:

Fluorescence quenching is a technique that has been successful at extracting information from several complex systems.[16-23] It was utilized here to investigate the host-guest relationship between the probe of interest and the large supramolecular assembly. For the experiments described in this work, intermolecular quenching was used with the physical addition of a quenching agent. In addition to molecular oxygen, amines, such as *N,N*-dimethylaniline (DMA), dimethylamine, trimethylaniline, nitromethane, diazabicyclo[2.2.2]octane, and dibutylamine are common fluorescence quenching agents. Quenchers, such as DMA, are small enough to penetrate the hydrogen bonded seams of the PgC_6 assembly and interact with the guest in a way that provides information about the accessibility and the nanoenvironment of the guest.

Quenching is a concept with a unique dynamic, consisting of decreasing the fluorescence emission of a species through collisional deactivation in the excited state (Equation 2.18).

$$Ar^* + Q \xrightarrow{k_q} [Ar^* \cdot Q] \qquad \textbf{Equation 2.18}$$

where Ar represents the fluorophore (in our case Ar is a polycyclic aromatic hydrocarbon, PAH), Q represents the quencher and k_q is the quenching rate constant. Quenching is known to be an adiabatic diffusion process. In the absence (Equation 2.19) or presence of the quencher (Equation 2.20), the change of the excited state species concentration is governed by the following equations:

$$\frac{d[Ar^*]}{dt} = k_a[Ar] - k_{fl}[Ar^*] - k_{ic}[Ar^*] - k_{nr}[Ar^*] \qquad \textbf{Equation 2.19}$$

$$\frac{d[Ar^*]}{dt} = k_a[Ar] - k_{fl}[Ar^*] - k_{ic}[Ar^*] - k_{nr}[Ar^*] - k_q[Q][Ar^*] \qquad \textbf{Equation 2.20}$$

where k_a, k_{fl}, k_{ic}, and k_{nr} correspond respectively to the rate constants of the absorbance, fluorescence, internal conversion, and nonradiative relaxation, k_q is the Stern-Volmer quenching constant, and [Ar*] and [Q]

are the fluorophore and the quencher concentration, respectively. Under steady-state conditions $\frac{d[Ar^*]}{dt} = 0$, where [Ar*] can be solved from Equation 2.19 and 2.20, as shown in Equation 2.21 and 2.22:

$$[Ar^*] = \frac{k_a[Ar]}{(k_{fl} + k_{ic} + k_{nr})} = F_0 \qquad \textbf{Equation 2.21}$$

$$[Ar^*] = \frac{k_a[Ar]}{(k_{fl} + k_{ic} + k_{nr} + k_q[Q])} = F \qquad \textbf{Equation 2.22}$$

Equation 2.19 represents [Ar*] when [Q] is not present; this quantity is directly proportional to the original fluorescence intensity, F_0, (Equation 2.7) before the addition of a quencher, and F is the fluorescence intensity in the presence of the quencher. Combining both Equations 2.21 and 2.22 gives the Stern-Volmer equation:

$$\frac{F_0}{F} = 1 + k_q[Q] \qquad \textbf{Equation 2.23}$$

The Stern-Volmer quenching constant, k_q, is the product of the true quenching constant and the excited state lifetime. This constant is determined from the slope of the line, which can be extrapolated from the

Stern-Volmer plot when the absorbance-corrected fluorescence intensity ratio versus the quencher concentration is plotted. The Stern-Volmer plot is created by a succession of experiments that slowly add a known quantity of quenching agent into the system of interest and measuring the fluorescence of each of the resulting solutions. Dynamic quenching can simply be described as the deactivation of a fluorescent species from the excited to the ground state. Static quenching is a reduction of the population of the excited state by a quenching agent.[1,3]

Differentiating between dynamic and static quenching (Scheme 2.2) is relatively easy even though both result in a linear Stern-Volmer plot. Ground-state quenching is static while dynamic occurs in the excited state. Temperature is a major factor in fluorescence quenching. Higher efficiencies in dynamic quenching are a result of higher temperatures that lower sample viscosities, promoting increased collisions. However, higher temperatures decrease the stability of the system in the ground state, resulting in lower static quenching rates. In the static mechanism, the fluorescence lifetime is also unaltered. Perturbations in the absorption spectrum, may reveal differences in static quenching since it is a ground state process and conversely, the

absorption is unaffected for the dynamic process, since it is occurs in the excited state.[1,3,4,19]

$$Ar + Q \rightarrow Ar - Q$$

Scheme 2.2 Static quenching mechanism and the formation of a nonradiative complex in the ground state.

Equations presented below show the ratio of $\frac{F_0}{F}$ in the Stern-Volmer depends on the concentration of the quencher.

$$K_{Ar...Q} = \frac{[Ar-Q]}{[Ar][Q]}$$

$$[Ar]_{total} = [Ar]_{free} + [Ar...Q]$$

$$K_{Ar...Q} = \frac{[Ar]_{total} - [Ar]_{free}}{[Ar]_{free}[Q]}$$

$$K_{Ar...Q} = \frac{[Ar]_{total}}{[Ar]_{free}[Q]} - \frac{[Ar]_{free}}{[Ar]_{free}[Q]}$$

$$K_{Ar...Q}[Q] = \frac{[Ar]_{total}}{[Ar]_{free}} - 1$$

$$1 + K_{Ar...Q}[Q] = \frac{[Ar]_{total}}{[Ar]_{free}} = \frac{F_0}{F}$$

$$\frac{F_0}{F} = 1 + K_{Ar...Q}[Q] \qquad \textbf{Equations 2.24}$$

The concentration affects the ratio in the dynamic quenching mechanism, where $K_{Ar...Q}$ is the association constant of the formation of the complex (Ar-Q).

V. Solvatochromism:

Solvatochromism simply means the system's color depends on the solvent system used. Spectroscopically, this property can be observed as intensity variations or a shift of the wavelength maxima in the absorbance and/or emission spectra. A positive wavelength shift is called a bathochromic or red shift, and a negative wavelength shift is called a hypsochromic or blue shift. This phenomenon is widely used to study the polarity of complex systems using dyes that systematically respond to polarity, such as pyrene or several of the Reichardt's dyes.[31]

Solvatochromism is well described in Figure 2.3, where it is shown how the ground and excited energy states change according to the polarity of the solvent. Nonradiative relaxation allows the solvent dipole moments to reorient and realign with the solute's excited-state dipole moment. Fluorescence emission from the solute occurs, allowing the reorientation of the solute prior to that of the solvent.

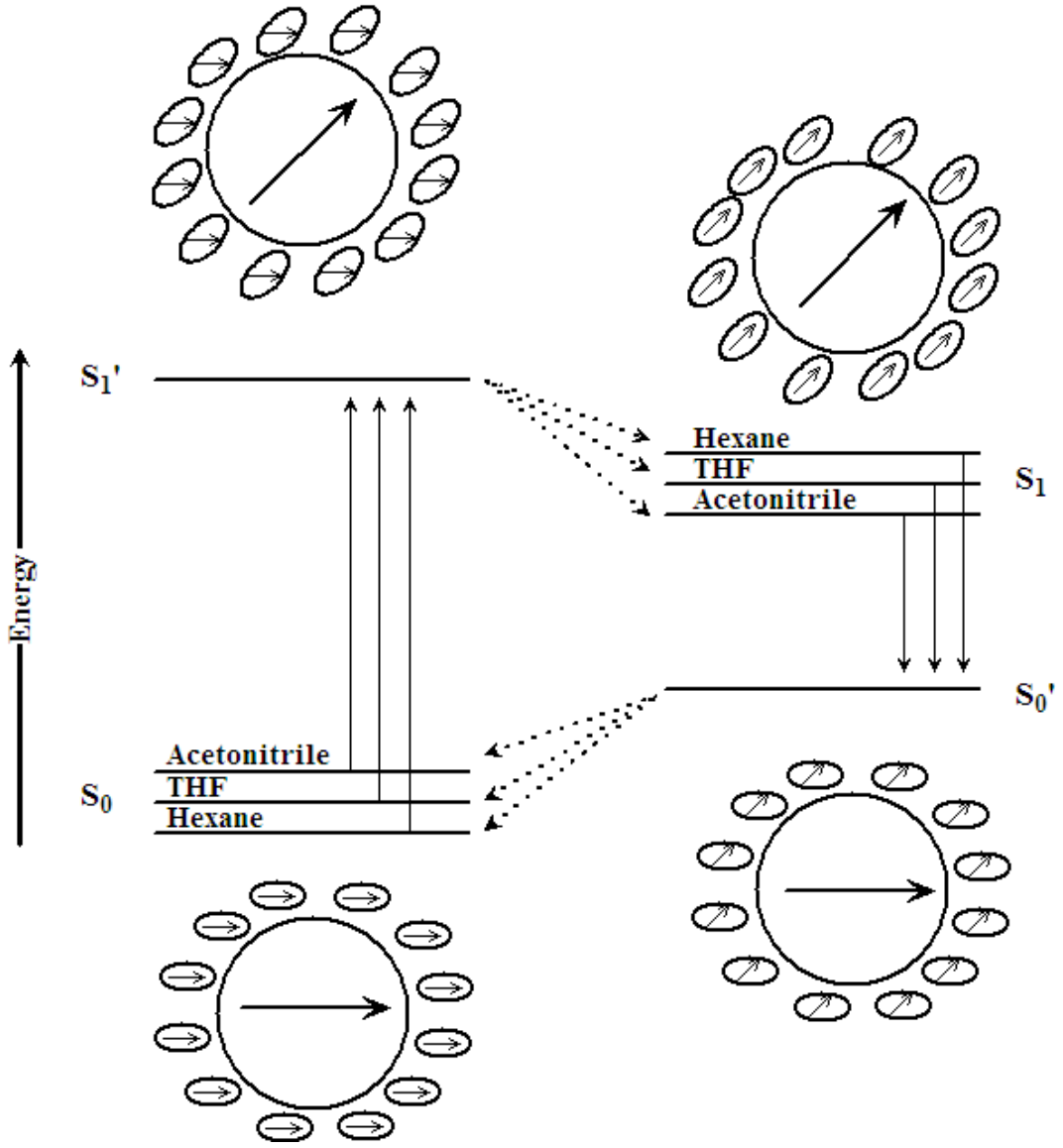

Figure 2.3 Modified Jabłoński diagram showing the relaxation process: dashed lines correspond to the non-radiative relaxation; solid lines represent the absorbance and the emission; circles correspond to the solute (large) and the solvent (small) electronic configurations with the arrows representing the dipole moment; S_0 represents the electronic ground state. (Redrawn from *Rutan et al.*)[38]

Solvents with higher polarity promote higher relaxation rates, since they have larger dipole moment that will further stabilize the electronic state. Solvatochromism is used to characterize and identify natural products, especially flavonoids where hydroxyl group substitution on the phenol rings affects the absorbance spectrum.[3]

Pyrene, pyrene butanol, and other reporter molecules are commonly used to investigate organized media.[32,33] An objective of this research is to refine the nature of the guest for optimal encapsulation within supramolecular nanocapsules. Pyrene and its derivatives are great candidates because their fine spectral structure changes with the polarity of the surrounding solvent. The parent fluorescent moiety, pyrene, present in these derivatives is able to indicate how polar the solvent is by using the ratio of the first versus the third vibronic band in the fluorescence emission. For example, in nonpolar hexane the ratio of I/III bands is 0.59, and it is 1.95 for very polar dimethyl sulfoxide.[34-36] Other pyrene derivatives show slight spectral perturbations when interacting with new environments.

VI. References:

(1) Lakowicz, J. R. *Principles of Fluorescence Spectroscopy*; Plenum Press: New York, 1983.

(2) Skoog, D. A.; Leary, J. A. *Principles of Instrumental Analysis*; 4th ed.; Saunders College Publishing: Fort Worth, 1992.

(3) Lakowicz, J. R. *Principles of Fluorescence Spectroscopy*; 2nd ed.; Kluwer Academic/Plenum Publishers: New York, 1999.

(4) Tucker, S. A. Ph.D. Dissertation, University of North Texas, **1994**.

(5) Smalley, M. B.; Shaver, J. M.; McGown, L. B. *Anal. Chem.* **1993**, *65*, 3466-72.

(6) Watkins, A. N.; Ingersoll, C. M.; Baker, G. A.; Bright, F. V. *Anal. Chem.* **1998**, *70*, 3384-3396.

(7) Gratton, E.; Jameson, D. M.; Hall, R. D. *Annu. Rev. Biophys. Bioeng.* **1984**, *13*, 105-24.

(8) Shaver, J. M.; McGown, L. B. *Anal. Chem.* **1996**, *68*, 611-20.

(9) Shaver, J. M.; McGown, L. B. *Anal. Chem.* **1996**, *68*, 9-17.

(10) Brochon, J. C.; Livesey, A. K.; Pouget, J.; Valeur, B. *Chem. Phys. Lett.* **1990**, *174*, 517-22.

(11) Geng, L.; McGown, L. B. In *SPIE Proceedings*; Lakowicz, J. R., Ed. Bellingham, WA, 1992; Vol. 1640.

(12) Shaver, J. M. Ph.D. Dissertation, Duke University, **1995**.

(13) McGown, L. B.; Hemmingsen, S. L.; Shaver, J. M.; Geng, L. *Appl. Spectrosc.* **1995**, *49*, 60-6.

(14) Livesey, A. K.; Skilling, J. *Acta Crystallogr., Sect. A: Found. Crystallogr.* **1985**, *A41*, 113-22.

(15) Foster, T. H.; Pearson, B. D.; Mitra, S.; Bigelow, C. E. *Photochem. Photobio.* **2005**, *81*, 1544-1547.

(16) Wade, D. A. Ph.D. Dissertation, University of Missouri - Columbia, **2000**.

(17) Wade, D. A.; Torres, P. A.; Tucker, S. A. *Anal. Chim. Acta* **1999**, *397*, 17-31.

(18) Wade, D. A.; Tucker, S. A. *Talanta* **2000**, *53*, 571-578.

(19) Richter-Egger, D. L. PhD. Dissertation, University of Missouri-Columbia, **2001**.

(20) Richter-Egger, D. L.; Landry, J. C.; Tesfai, A.; Tucker, S. A. *J. Phys. Chem. A* **2001**, *105*, 6826-6833.

(21) Richter-Egger, D. L.; Tesfai, A.; Tucker, S. A. *Anal. Chem.* **2001**, *73*, 5743-5751.

(22) Goodpaster, J. V.; McGuffin, V. L. *Anal. Chem.* **2000**, *72*, 1072-1077.

(23) Goodpaster, J. V.; McGuffin, V. L. *Anal. Chem.* **2001**, *73*, 2004-2011.

(24) Dalgarno, S. J.; Bassil, D. B.; Tucker, S. A.; Atwood, J. L. *Angew. Chem., Int. Ed. Engl.* **2006**, *45*, 7019-7022.

(25) Chuang, T. J.; Cox, R. J.; Eisenthal, K. B. *J. Am. Chem. Soc.* **1974**, *96*, 6828-31.

(26) Crawford, M. K.; Wang, Y.; Eisenthal, K. B. *Chem. Phys. Lett.* **1981**, *79*, 529-533.

(27) Gusten, H.; Meinsner, R.; Schoof, S. *J. Photochem.* **1980**, *14*, 77.

(28) Okada, T.; Fujita, T.; Kubota, M.; Masaki, S.; Mataga, N.; Ide, R.; Sakata, Y.; Misumi, S. *Chem. Phys. Lett.* **1972**, *14*, 563.

(29) Wang, Y.; Crawford, M. C.; Eisenthal, K. B. *J. Am. Chem. Soc.* **1982**, *104*, 5874-5878.

(30) Wang, Y.; Crawford, M. K.; Eisenthal, K. B. *J. Phys. Chem.* **1980**, *84*, 2696-2698.

(31) Reichardt, C. *Chem. Rev.* **1994**, *94*, 2319-2358.

(32) Dumas, D.; Muller, S.; Gouin, F.; Baros, F.; Viriot, M.-L.; Stoltz, J.-F. *Arch. Biochem. Biophys.* **1997**, *341*, 34-39.

(33) Ribou, A.-C.; Vigo, J.; Salmon, J.-M. *Photochem. Photobio.* **2004**, *80*, 274-280.

(34) Acree, W. E., Jr.; Tucker, S. A.; Fetzer, J. C. *Poly. Arom. Compd.* **1991**, *2*, 75-105.

(35) Dong, D. C.; Winnik, M. A. *Photochem. Photobio.* **1982**, *35*, 17-21.

(36) Dong, D. C.; Winnik, M. A. *Can. J. Chem.* **1984**, *62*, 2560-5.

(37) Kauffman, J. F.; Khajehpour, M.; Saleh, N. i. *J. Phys. Chem. A* **2004**, *108*, 3675-3687.

(38) Cecil, T. L.; Rutan, S. C. *Anal. Chem.* **1990**, *62*, 1998-2004.

Chapter 3: Materials and Methods

I. Materials:

Neat solvents and chemicals were obtained in the purest commercially available form and used as received. The most commonly used materials that resulted in successful outcomes are as follows: pyrene butanol (PyBt), 9-anthracene carboxylic acid (99% pure), 1,4-bis[5-phenyl-2-oxazolyl]benzene (POPOP), cyclohexane (99% A.C.S. spectrophotometric grade), *N,N*-dimethylaniline (DMA, 99.7% redistilled), pyrene (98%), and pyrene butyric acid (PBA) from Sigma-Aldrich, Saint Louis, MO; acetonitrile (ACN, HPLC grade), hexane (HEX, optima grade), ethanol (A.C.S. grade), methanol (HPLC grade), and tetrahydrofuran (THF, certified grade) from Fisher-Scientific, Fair Lawn, NJ; *C*-hexylpyrogallol[4]arenes[1,2] (PgC_6) was synthesized according to literature procedures.[1-3] Several other guest molecules were examined and are listed in tables later in this Chapter with their properties of interest in this work. General experimental methodology is presented here with details specific to each guest further delineated within the respective chapters.

Figure 3.1 illustrates the synthesis of the tetramers or building blocks, where six of the latter self-assemble to form *C*-hexylpyrogallol[4]arenes nanocapsules. The synthesis of the building blocks were performed as follows: ten grams (0.0725 mol) of pyrogallol (Acros Organic, Morris Plains, NJ; MW = 126.11 g/mol) and 1107 mL of heptaldehyde (Sigma-Aldrich, Saint Louis, MO; density = 0.82, MW = 114 g/mol) were dissolved in the minimum amount of ethanol, and the reflux process was started. Just before the solution boiled, the heat was removed, and 5 mL of the acid (1 mL of concentrated chloric acid per 2 g of pyrogallol) were added. The heat was returned, and the reaction was then refluxed for 2-24 hours until precipitate appears.

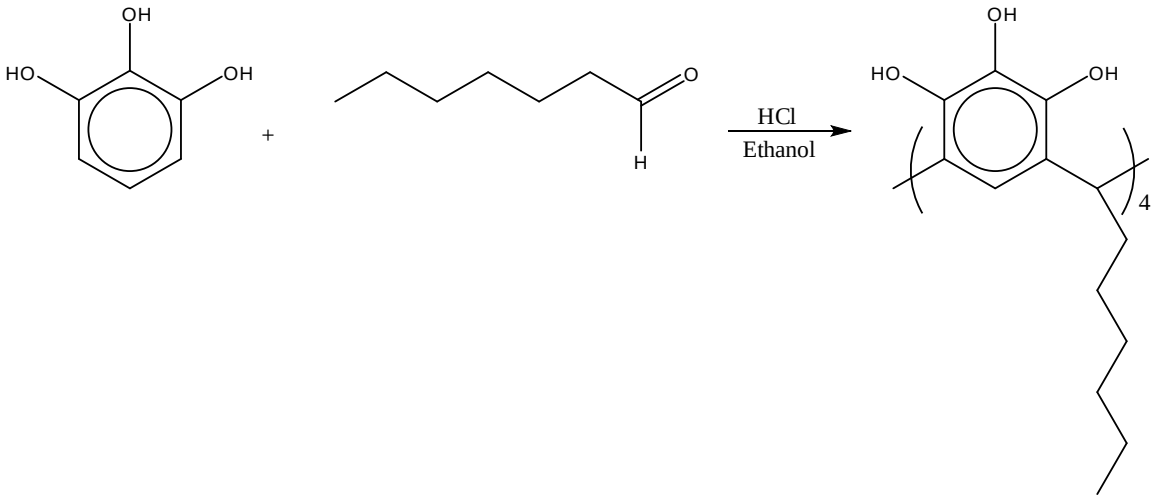

Figure 3.1 PgC_6 building block's synthesis from Pg and heptaldehyde.

The self-assembly of hydrogen bonded supramolecular complexes and encapsulation of a guest was facilitated by sonication of a saturated solution of *C*-alkylpyrogallol[4]arenes (PgC_n) and the guest in ACN: 60 mg of PgC_n were added to 6 mL of saturated guest solution in ACN in a 20 mL screw top scintillation vial; and the mixture was heated with a hot plate (below the boiling stage) until the powder totally dissolved. The self-assembly of metal-containing supramolecular complexes begins with *C*-propan-3-ol pyrogallol[4]arene[4] treated with four parts $Cu(NO_3)_2 \cdot 3H_2O$ in a solution of acetone and water. Red crystals should form in ~24 hrs.

The vial contents were allowed to sit for two days, while the color and possible crystal formation were monitored. Most of the time crystals formed in the time period allotted. This was especially true for the $CuPgC_n$ assemblies. However, if in two days, no crystals appeared, a slow evaporation technique was performed. This was generally needed for PgC_n assemblies. In this technique, the cap of the vial was kept half open or a foil with a small hole in it was placed on the vial in order to evaporate the solvent slowly. As previously reported, crystals were characterized by single crystal X-ray diffraction and proton nuclear magnetic resonance (^{1}H-NMR) spectroscopy.[5]

Stock solutions (~10^{-4} M) of the free fluorophore and the encapsulated complex were prepared by dissolving the dye or a single crystal of the latter in ACN. To confirm probe occupation within the nanocapsules, crystals were irradiated with a Spectroline® UV lamp (254 and 365 nm) to observe the fluorescence. Diluted samples were prepared by quantitatively transferring known aliquots of the stock solutions into volumetric flasks and diluting to volume. The final concentration of the fluorophore in any solvent system was optically dilute (~10^{-6} M). Samples were examined immediately upon mixing, with the exception of the time-lapse studies that were stored in the dark in sealed vials, and were interrogated at room temperature (20-25 ˚C).

Table 3.1 contains the fluorescent reporter molecules that have been successfully encapsulated in a supramolecular assembly with the exception of 9-anthracene carboxylic acid, which was inconclusive due to lack of crystallization. Two probes that have evidence of encapsulation but at the present are too highly disordered to determine definitively are *p*-nitro aniline and 2,3-diaminonaphthalene. Other fluorescent probes that were investigated for encapsulation purposes in the $CuPgC_3$ and PgC_6 nanocapsules are listed in Table 3.2 along with any functional group of interest.

Fluorescent Reporter	λ_{EX}	λ_{EM}
Pyrene[6]	338	371, 382, 391, 413
Pyrene butanol	325	377, 387, 397, 420
Pyrene butyric acid	338	375, 386, 394, 416
9-anthracene carboxylic acid	334	390, 418, 440, 460
p-Nitro analine	370	423
2,3-Diaminonaphthalene	340	383

Table 3.1 Fluorescence excitation and the major emission wavelengths of the fluorescent reporter molecules used for encapsulation in the PgC_6 nanocapsule.

Table 3.3 contains all of the probes that were only utilized as encapsulation probes in the $CuPgC_3$ nanocapsule and not for ligand attachment. The samples were allowed to age after dissolving the crystal; the process took place in a dark place at ambient temperature. The purpose of the aging process is to study the robustness of the host-guest complex.

Fluorescent dyes	**Functional groups**
Fluorescein	-OH
Pyrene Butyric Acid	-OH, -COOH
Pyrene Carboxylic Acid	-OH, -COOH
2,3-Dihydroxybenzoic Acid	-OH, -COOH
1-Pyrenedecanoic Acid	-OH, -COOH
1-Pyrenedodecanoic Acid	-OH, -COOH
BODIPY®	multiple
8-Hydroxyquinoline	-OH, $-NR_2$
Thymol blue	-OH, $-SR_2$
Titan Yellow	$-SR_2$, $-NR_2$, -NRH
Anthraquinone Violet	$-SR_2$, -NRH
Methylene Blue	$-SR_2$, $-NR_2$
Congo Red	$-SR_2$, $-NR_2$, $-NH_2$
Crystal Violet	$-NR_2$
Brilliant Cresyl blue	$-NR_2$, $-NH_2$
Azure A	$-SR_2$, $-NR_2$, $-NH_2$
Methyl Green	$-NR_2$
Et-30	$-NR_2$
Neutral Red	$-NR_2$, -NRH, $-NH_2$
Basic Fushin	$-NH_2$
Rhodamine 123	-NRH, NH_2, $-COOCH_3$
Rhodamine 6G	$-NR_2$, -NRH, $-COOCH_3$
Fluorescein Diactetate	$-COOCH_3$
Calcein	$-COOCH_3$

Table 3.2 Fluorescent probes of interest with germane functional groups noted.

Fluorescent Dye	**Functional Group**
Naphthalene	none
Acenaphthene	none
Fluorene	none
Phenanthrene	none
Pyrene	none
2-Acetylphenanthrene	$-COCH_3$
3-Acetylphenanthrene	$-COCH_3$

Table 3.3 Fluorescent probes utilized for encapsulation in the $CuPgC_3$ nanocapsule.

II. Instrumental Measurements:

All spectra were collected in 1 cm^2 Suprasil quartz cuvettes (Hellma, Forest Hills, NY), and absorption spectra were recorded on a Hitachi U-3000 double-beam spectrophotometer (Hitachi Instruments, Danbury, CT), with a scan rate of 120 nm/min, a slit width of 1 nm, and a thermostated cell temperature of 25 ˚C. Spectra were blank corrected

for the possible absorption of unoccupied nancapsule in solution and the quenchers used, though little to no background signal due to the unoccupied nanocapsules in solution was apparent in the wavelength regions of interest.

Fluorescence spectra were measured with a SLM 48000 DSCF/MHF spectrofluorometer (Jobin Yvon, Edison, NJ) at a thermostated cell temperature of 25 ˚C. The excitation source for fluorescence emission and liftetimes was Kimmon (Tokyo, Japan) He-Cd laser excitation source at 325 nm. Emission slit widths were set at 2.5 nm. Excitation wavelength was chosen due to proximity to the optimal absorbance. All emission spectra are blank corrected. When necessary, inner-filter corrections where applied (Equation 3.1)[7].

$$F_{cor} = F_{obs}\left[\frac{2.303A_{exc}(0.55-0.45)}{10^{-A_{exc}0.45}-10^{-A_{exc}0.55}}\right] \qquad \textbf{Equation 3.1}$$

where F_{cor} and F_{obs}, represent the corrected and the observed fluorescence intensity, respectively, A_{exc} is the optimal absorbance

wavelength used for the excitation of the sample. The number 0.55 and 0.45 are the typical cell geometry values that are illustrated from Figure 3.1, where X = U = 0.45 cm and Y = V = 0.55 cm.[8] The correction factor, $F_{prim} \approx 10^{0.5Aexc}$, is equal the ratio of F_{cor} and F_{obs} (Equation 3.2):

$$F_{prim} = \frac{F_{cor}}{F_{obs}} \qquad \textbf{Equation 3.2}$$

For solution measurements a 90º excitation-emission geometry is used, as the signal to noise ratio is maximized. Primary inner-filtering is a self-quenching mechanism, and secondary inner-filtering that may occur also is a self-absorption mechanism.[7,8,10-12] Inaccurate conclusions can be drawn and quantitative concentration comparison would be impossible upon failure to correct the emission spectra.

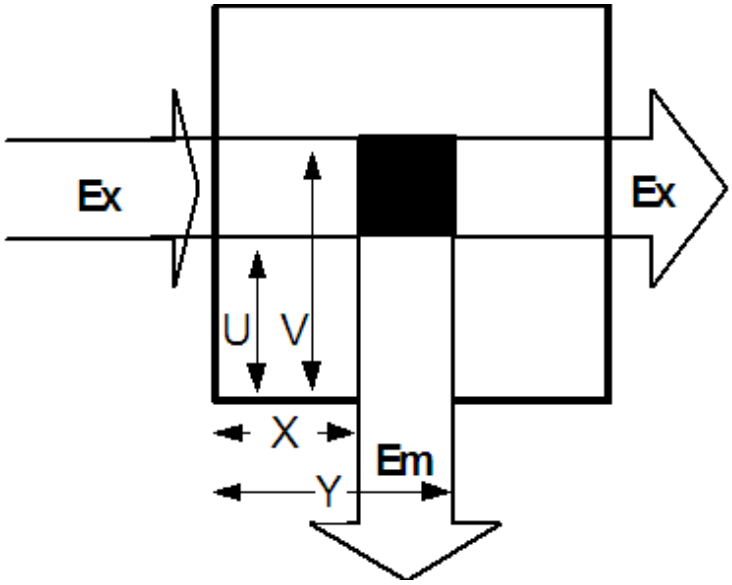

Figure 3.2 Reproduced representation of the effect of sample geometry, and the dimensions used for the inner-filter correction.[7]

III. Fluorescence Lifetime Measurements:

Lifetimes were collected in the frequency domain[13] on a SLM 48000 DSCF/MHF spectrofluorometer, with multiharmonic, Fourier transform (MHF) phase-modulation capabilities. The excitation source was a Kimmon He-Cd laser excitation source operated at 325 nm and 10 mW. In MHF mode, however, only a small fraction of the excitation power interrogates the sample. A base frequency of 4.0 MHz and a

cross-correlation frequency of 7.000 Hz were used, ten pairs of sample-reference measurements were collected in triplicate for each sample, and each measurement contained 50 internal averages. The lifetime reference (τ_{ref} = 1.34 ns) was POPOP in ethanol. The following filter was employed for PyBt emission collection: a 400 nm (80 nm band pass: 03 FIB 002 Melles Griot). Lifetime data were analyzed by the SLM nonlinear least squares data package provided by the manufacturer.

IV. References:

(1) Cave, G. W. V.; Antesberger, J.; Barbour, L. J.; McKinlay, R. M.; Atwood, J. L. *Angew. Chem., Int. Ed.* **2004**, *43*, 5263-5266.

(2) Gerkensmeier, T.; Iwanek, W.; Agena, C.; Frohlich, R.; Kotila, S.; Nather, C.; Mattay, J. *Eur. J. Org. Chem.* **1999**, 2257-2262.

(3) Syage, J. A.; Felker, P. M.; Zewail, A. H. *J. Chem. Phys.* **1984**, *81*, 2233-56.

(4) Gibb, B. C.; Chapman, R. G.; Sherman, J. C. *J. Org. Chem.* **1996** *61*, 1505-1509.

(5) Dalgarno, S. J.; Bassil, D. B.; Tucker, S. A.; Atwood, J. L. *Angew. Chem., Int. Ed. Engl.* **2006**, *45*, 7019-7022.

(6) Tucker, S. A. Ph.D. Dissertation, University of North Texas, **1994**.

(7) Lakowicz, J. R. *Principles of Fluorescence Spectroscopy*; Plenum Press: New York, 1983.

(8) Wade, D. A. Ph.D. Dissertation, University of Missouri - Columbia, **2000**.

(9) Holland, J. F.; Teets, R. E.; Kelly, P. M.; Timnick, A. *Anal. Chem.* **1977**, *49*, 706.

(10) Parker, C. A.; Barnes, W. J. *Analyst* **1957**, *82*, 606.

(11) Yappert, M. C.; Ingle, J. D. *Appl. Spectrosc.* **1989**, *43*, 759.

(12) Gupta, D.; Basu, S. *J. Photochem.* **1975**, *4*, 307-8.

(13) Dalgarno, S. J.; Tucker, S. A.; Bassil, D. B.; Atwood, J. L. *Science* **2005**, *309*, 2037-2039.

Chapter 4: Copper Containing Capsules

I. Metal Containing Capsules:

Supramolecular chemists are always trying to find new and better nanocapsules; 'better' entailing an array of different characteristics. In general, capsules that include metal ions in place a some of the hydrogen bonds (H-bonds) are more stable in the solid state than capsules only containing H-bonds. These capsules are readily soluble in a variety of solvents and are expected to retain their superior stability over the hydrogen-bonded capsules in solution, as well. However, solution-state chemistry of the metal-containing capsules is all but nonexistent, and therefore, these properties are as of yet undetermined.

A copper-containing nanocapsule that is analogous to the C-hexylpyrogallol[4]arene (PgC_6) was used for the work described herein. The hexameric hydrogen bound PgC_6 capsule is seamed together by 72 H-bonds. Conversely, the copper capsule has 48 H-bonds with 24 Cu(II) metal ions. These copper ions are found to be in the form of 96 Cu-O coordination bonds. Oxygen atoms from the marcocycle's upper rim occupy all four equatorial positions on each copper ion.[1] An X-ray crystal

structure of the copper propylpyrogallol-4-arene, $CuPgC_3$ is shown in Figure 4.1. This capsule was investigated in solution, and the following results were obtained.

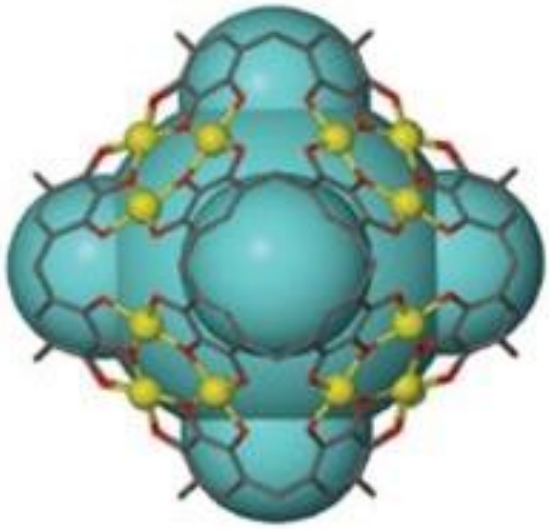

Figure 4.1 X-ray crystallographic representation of the $CuPgC_n$ nanocapsule. The copper metal ions are in yellow, and the H-bonds are in red.

II. Probe Attachment:

Since the $CuPgC_3$ nanocapsules are analogous to the hydrogen-bound PgC_6, the comparative abilities to house guest molecules was of interest. With these materials, internal (encapsulated) and external

(ligand attachment) probe association was thought probable. Encapsulation would allow for the interior of the nanocapsule to be explored and the host-guest properties to be determined. External attachment of a fluorophore would allow for the study of external surface microenvironment, neighboring interactions with other nanocapsules, etc. Non-metal nanocapsules, with fluorophores dangling from the nonpolar tails through covalent bonding,[2] have been noted in the literature, but surface attachment has not. The advantage of such is the close proximity to the supramolecular structure.

Initial studies focused on externally attaching a probe. Through ligand attachment, the surface chemistry of the nanocapsule could be examined. Due to the affinity of copper for hydroxyl, amine, amide, and sulfur containing functional groups, any potential probes containing one or more of these groups were selected when possible. Table 4.1 contains the dyes that were initially tested with the $CuPgC_3$ nanocapsule. The first four dyes are common fluorophores that contain hydroxyl functional groups (OH). These four dyes, with the exception of PBA, do not have the functionality contained within a long carbon chain tail. Pyrene butyric acid was included to determine if functionality on a carbon chain could facilitate attachment to the copper metal ions at the nanocapsule

surface. There was concern that surface crowding, due to the short propyl carbon chains on the pyrogallol, might be an issue. In addition to PBA with a four-carbon tail, the last three dyes in Table 4.1 have very long carbon chains. The BODIPY® dye in particular is specifically made to mimic and penetrate lipid layers in biological samples.[3-7]

While all seven of these fluorophores had the necessary functional group, their solubility in the necessary assembly solvent, as noted in Table 4.1, was not ideal. The $CuPgC_3$ nanocapsule is slightly insoluble in water and soluble in other polar solvents like methanol only over an extended time period. However, insolubility of a fluorophore is frequently used to drive association with macromolecules.[8] While great things were expected for these seven dyes, no crystals or solid precipitate were produced in any of the samples. Slight color changes were noted for fluorescein, phenol blue, and Nile red, indicating a possible interaction between the copper and the probe. Solutions containing the long-chain dyes were colorless, indicating no reaction had taken place between the copper and the probe. Since discernable results were not produced and the cost of the probes, which are added in excess, is a significant limitation, the ligand attachment process had to be simplified. If successful, the system of interest could be scaled back up.

Fluorescent Probe	**Recommended Solvent**
Fluorescein	Methanol
Phenol Blue	Tetrahydrafuran, Water
Nile Red	Water
Pyrene Butyric Acid	ACN
1-Pyrenedecanoic Acid	Water, Dimethyl sulfoxide
1-Pyrenedodecanoic Acid	Water, Dimethyl sulfoxide
BODIPY®	Water, Dimethyl sulfoxide

Table 4.1 Fluorescent dyes and the recommended solvents based on solubility.[6]

III. External Attachment:

III.1 Catechol and Copper:

To simplify the $CuPgC_3$ nanocapsule, it was broken down into its parts. As shown below in Figure 4.2, catechol is remarkably similar to the pyrogallol building block of the nanocapsule. Therefore, it was used along with various copper species in an attempt to mimic nanocapsule

attachment. The formation of simplified complexes would afford the same chemical functionality as the more complex $CuPgC_3$ marcocycles possess. By producing these simplified complexes and using them to compare various probes, resulting in less waste of the more valuable nanocapsules and minimization of the amount of fluorophore consumed.

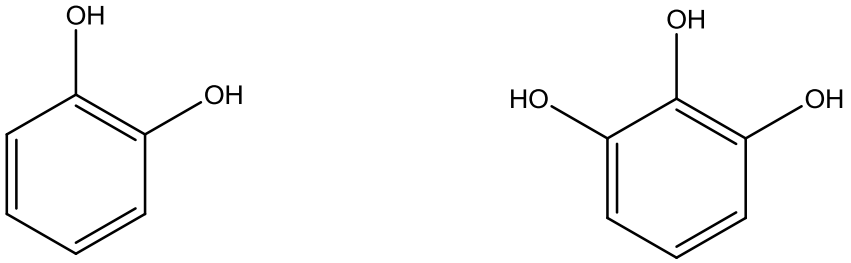

Figure 4.2 Structural comparisons between catechol and pyrogallol.

Four copper compounds were used to form the complex with catechol: copper acetate, copper chloride, copper sulfate, and copper nitrate. The only solution to produce any precipitate was copper sulfate. This small amount of precipitate was then added to a solution of fluorescein in methanol and to a solution of pyrene butyric acid in ethyl acetate. No discernable chemical reactions were observed. This could be due to the precipitate that was used, as the reaction of catechol and

copper sulfate was not verified. Numerous solutions containing catechol and the various copper compounds were prepared, but no precipitate was reproduced. Since the only combination of catechol and copper compound that even remotely suggested a reaction occurred did not produce any feasible results after multiple attempts and could not be reproduced, the focus returned to the $CuPgC_3$ nanocapsule.

III.2 Solvent Stability:

The $CuPgC_3$ capsule was tested for solvent stability. These metal-containing assemblies are expected to have higher stability in a greater range of solvents than the PgC_6 nanocapsules, which are limited to nonpolar and slightly polar solvents. Nine solvents that are common to both synthetic and fluorescence work were tested. Solutions consisted of 0.4 - 0.6 mg of $CuPgC_3$ in 3 mL of neat solvent. Observations of the solutions were taken over three days, every morning and afternoon. Three of the solutions had no change in the time period allotted. These were the extreme right and left of the polarity scale: water, toluene, and hexane. In these solvents, the capsule was visibly insoluble with no solution color change observable over the three-day period. Dimethyl

sulfoxide, ethanol, and methanol all had a slight solution color change the first day. By the second day, most of the $CuPgC_3$ was dissolved and was completely solubilized by the third day. Acetone and tetrahydrafuran had no noticeable change the first day, but by the third day $CuPgC_3$ was slowly going into solution. The last solvent, acetonitrile (ACN) is the most common solvent used with these capsules, and surprisingly the outlier when compared to solvents with similar polarity solvents. Initially, no color change was observable for $CuPgC_3$ in ACN; however, when the solutions were checked six or seven hours later, the capsule was completely dissolved with a slight color change. These results showed that while ACN would be the best solvent to continue using with the capsules, if needed, a moderately polar solvent could be utilized.

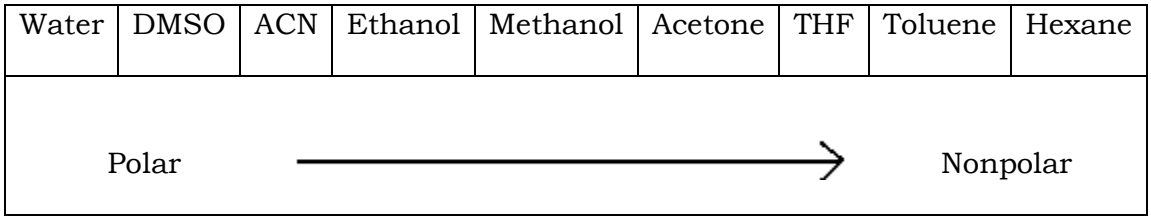

Figure 4.3 Polarity scale of the solvents used to determine solubility of $CuPgC_3$.

III.3 Functional Groups:

The primary functional groups initially investigated were hydroxyl and carboxylic acids, but these are not the only functional groups that could possibly bind to copper. As mentioned previously, other probable functional groups are amines, amides, ketones, aldehydes, and sulfur-containing compounds. Table 4.3 has a complete list of the attempted dyes and the types of functional groups they contain.

Results from these studies were generally inconclusive and not very promising. Some solutions had a color change, indicating some sort of interaction with the copper ion. This potential interaction was only visibly detected (color change); solid product of any type was not observed. The concentrations of the dyes were increased and for the majority of the dyes, solid precipitate of any kind still did not form. One of the exceptions, 9-anthracene carboxylic acid did produce a precipitate. The precipitate was filtered and the remaining filtrate was set aside to determine if more precipitate (second generation) would form. A small amount of the first-generation precipitate was dissolved and interrogated using fluorescence spectroscopy. The fluorescence emission spectrum measured is seen in Figure 4.3.

Fluorescent Dyes	**Functional Groups**
Fluorescein	-OH
Pyrene Butyric Acid	-OH, -COOH
Pyrene Carboxylic Acid	-OH, -COOH
2,3-Dihydroxybenzoic Acid	-OH, -COOH
9-Anthracene Carboxylic Acid	-OH, -COOH
8-Hydroxyquinoline	-OH, $-NR_2$
Thymol Blue	-OH, SR_2
Titan Yellow	$-SR_2$, $-NR_2$, -NH
Anthraquinone Violet	$-SR_2$, -NRH
Methylene Blue	$-SR_2$, $-NR_2$
Congo Red	$-SR_2$, $-NR_2$, $-NH_2$
Crystal Violet	$-NR_2$
Brilliant Cresyl Blue	$-NR_2$, $-NH_2$
Azure A	$-SR_2$, $-NR_2$, $-NH_2$
Methyl Green	$-NR_2$
Et-30	$-NR_2$
Neutral Red	$-NR_2$, -NRH, $-NH_2$
Basic Fushin	$-NH_2$
Rhodamine 123	-NRH, NH_2, $-COOCH_3$
Rhodamine 6G	$-NR_2$, -NRH, $-COOCH_3$
Fluorescein Diactetate	$-COOCH_3$
Calcein	$-COOCH_3$

Table 4.2 Fluorescent probes pertinent to the study and the functional groups they contain

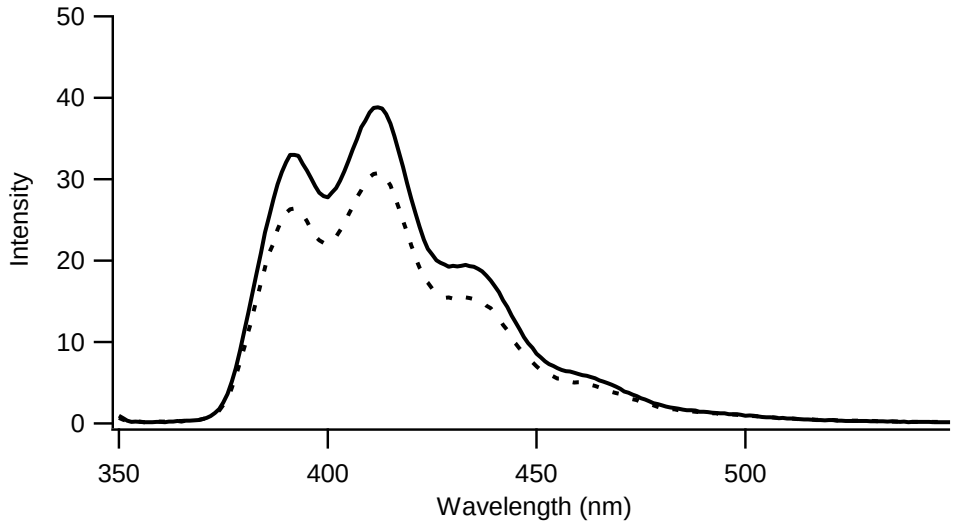

Figure 4.4 Representative fluorescence emission spectra of three replicates for first- (solid) and second-generation precipitate (dashed) of 9-anthracene carboxylic acid with $CuPgC_3$.

As noted in Figure 4.3, the first- and second-generation precipitate has the emission fingerprint of anthracene – the series of well-defined vibronic bands. While this appeared promising, it could not be determined whether the precipitate examined was in fact dye coordinated to or interacting with the capsule or if it was just re-solidified dye. Recrystallization efforts were unsuccessful and the solution was lost to evaporation. Recreation of the same experiment with a 9-anthracene carboxylic acid solution did not successfully produce precipitate.

IV. Internal Association:

IV.1 Polycyclic Aromatic Hydrocarbons:

After repeating the experiments, varying the concentration of the dye in solution for ligand attachment of a fluorescent dye molecule to the copper ion, and having no successful results, the focus shifted to encapsulation. Additional dyes were tested to enhance the chances of encapsulation. Along with all the dyes listed in Table 4.3, some polycyclic aromatic hydrocarbons (PAH) were also used. They are listed in Table 4.4. Again, results were less than promising. A few solutions that exhibited color changes previously were seen again. The PAH containing solutions had no color change, and no precipitate was observed.

Fluorescent Dye	**Functional Group**
Naphthalene	None
Acenaphthene	None
Fluorene	None
Phenanthrene	None
Pyrene	None
2-Acetylphenanthrene	$-COCH_3$
3-Acetylphenanthrene	$-COCH_3$

Table 4.3 PAHs with germane functional groups noted.

IV.2 Dialysis:

Since a color change indicated that some sort of interaction was occurring between the $CuPgC_3$ nanocapsule and some of the fluorescent dyes and no crystallization had occurred, an attempt to isolate and concentrate the potential complex was undertaken. Stock solutions of pyrene and $CuPgC_3$ in various solvents were made and then analyzed by fluorescence spectroscopy (Figure 4.4). Once emission measurements were complete, the solutions were dialyzed and then re-analyzed. The hope was that any excess dye in the solution would be, through the process of osmosis, leached from the sample bag. External solvent could then be replaced, until what remained in the dialysis bag would be the $CuPgC_3$ capsule and any dye associated in it. This solution could then be analyzed and/or set aside for recrystallization.

The solvent in the dialysis chamber was changed daily along with the daily sampling and analysis. As shown in Figure 4.4, the intensity of pyrene in solution decreases rapidly over the time period listed. Moreover, the entire emission spectrum blue shifts with time. Typically the first vibronic band of pyrene is *circa* 370 nm, as seen prior to

dialysis. Post dialysis, the spectral perturbations are obvious and significant, in all three spectra.

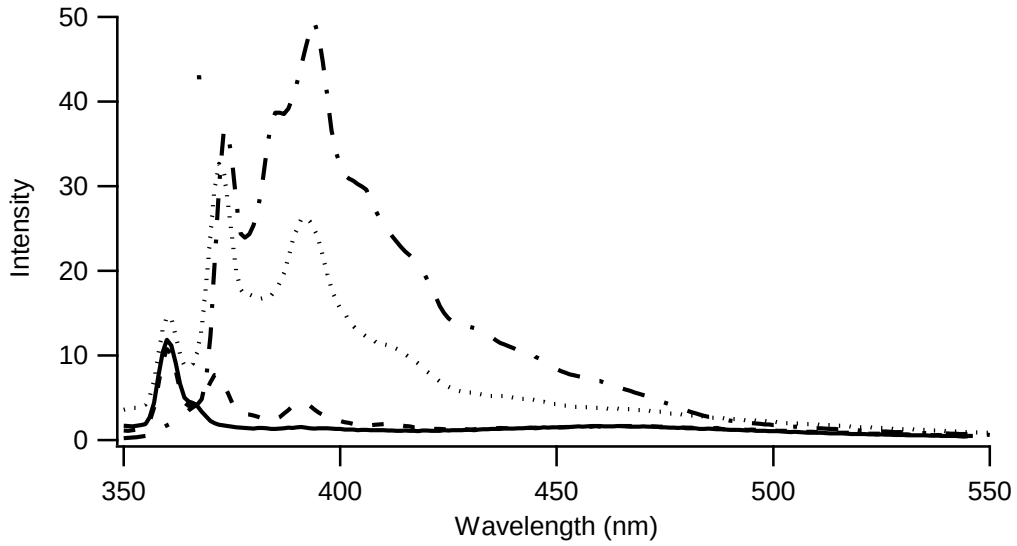

Figure 4.5 Representative fluorescence emission spectra of three replicates of $CuPgC_3$ and pyrene in methanol before dialysis (dot/dash), day 1 (dotted), day 3 (dashed), and day 6 (solid).

Pyrene is a solvent polarity probe, and the ratio of the first and third vibronic bands (PY I/III) is used to determine the microenvironmental polarity. However, in this case, the spectral shifts prevent such determination from being valid and meaningful. The addition of fresh solvent displaced any excess dye and, as observed above, any pyrene that had attached itself to the capsule or had been encapsulated. The association, if any, was not strong or stable enough under these conditions. This does not disprove the fact that there could

be interactions between the copper and the pyrene in solution. It just shows that for the solution-state fluorescence studies, nothing could be definitively determined about the visible observations, i.e., color change. The same experiment was executed using crystal violet, aminopyrene, and rhoamine-123 dyes, and similar results were observed.

V. Conclusions:

$CuPgC_n$ is a more stable nanocapsule than the previously mentioned species containing only H-bonds. Even though its stability in a variety of solvents and the presence of metal ions make it a more desirable nanocapsule for some applications in supramolecular chemistry, the solution-state understanding of such systems presented significant challenges. As these studies have shown, it is difficult to attach a fluorescent dye molecule to the copper nanocapsule; difficult but hopefully, not impossible. Additional research into fluorescent dyes that would form a chelate with the copper ion could reveal possible surface binding of said dye to the nanocapsule. Since all of the dyes used for the above studies had the acceptable functional groups, but did not appear to allow the chelate to form, it is possible that the orientation of

the functional group on the fluorophore is a viable reason why no discernable results were seen in the attempts to attach a ligand to the $CuPgC_3$ nanocapsule. Another reason could simply be that the copper is a known quencher of fluorescence, which makes any observation via fluorescence difficult to carry out.[9]

Future studies into these copper containing nanocapsules will utilize fluorescent chelaters (e.g., calcein blue and Fluo-3AM). Along with chelaters, probes that contain metal ions will used in the hydrogen bound nanocapsules to observe whether the metal ion related to the probe displaces some of the H-bonds and forms a complex. It will be interesting to find out if the metal ion of the probe aids in the encapsulation process.

VI. References:

(1) McKinlay, R. M.; Cave, G. W. V.; Atwood, J. L. *PNAS* **2005**, *102*, 5944-5948.

(2) Barrett, E. S.; Dale, T. J.; Rebek, J. R. *Chem. Commun.* **2007**, 4224-4226.

(3) Thompson V. F.; Saldaña S.; Cong J.; Goll D. E. *Anal. Biochem.* **2000**, 279, 170-178.

(4) Hara T.; Hirasawa A.; Sun Q.; Koshimizu T. A.; Itsubo C.; Sadakane K.; Awaji T.; Tsujimoto G.; *Mol. Pharmacol.* **2009**, 75, 85-91.

(5) McEwen D. P.; Gee K. R.; Kang H. C.; Neubig R. R.; *Anal. Biochem.* **2001**, 291, 109-117.

(6) Haugland, R. P., *The Handbook: A Guide to Fluorescent Probes and Labeling Technologies*. 10th ed.; Invitrogen Corp: 2005.

(7) McEwen D. P.; Gee K. R.; Kang H. C,; Neubig R. R.; *Anal. Biochem.* **2001**, 291, 109-117

(8) Morgan, Elizabeth J.; Rippey, Julie M.; Tucker, Sheryl A. *Appl. Spectrosc.* **2006**, *60*, 551-559.

(9) Lakowicz, J. R. *Principles of Fluorescence Spectroscopy*; Plenum Press: New York, 1983.

Chapter 5: Encapsulation of Pyrene Butanol

I. Introduction:

Previous studies of hexylpyrogallol[4]arene (PgC_6) nanocapsules employed a series of polycyclic aromatic hydrocarbons (PAHs) as guests.[1] These reporter molecules were chosen because of their spectroscopic probe properties and ability to fit into the nanocapsule interior. To date, encapsulation attempts have utilized many different fluorescent probes, most of which are listed in Table 5.1. Two of the probes, 2,3-diaminonapthalene, and *p*-nitro aniline, are waiting to be resolved via X-ray

Fluorescent Probes	
n-Phenyl-1-napthylamine	*p*-Nitro Aniline
2,3-Diaminonapthalene	Thymol Blue
Phenol Blue	Basic Fuschin
Nile Red	Bromopyrene
Acrylodan	Aminopyrene
Fluorescein Diacetate	Nitropyrene

Table 5.1 Possible guest molecules for the PgC_6 nanocapsule.

diffraction. There is evidence of possible encapsulation; however, at this time, there is no definitive evidence of entrapment. As mentioned previously, the results obtained for pyrene and its derivatives directed the most recent research presented here (Figure 5.1).[1]

In solution, pyrene encapsulation in the PgC_6 was found to be unstable, and the lack of solid-state crystal data gave little insight into the host-guest association. On the other hand, pyrene butyric acid (PBA) was successfully encapsulated and found to be stable in both solid and solution state.[2] Given that the differences between the guests is only the addition of a functional group, this research focused on answering the question about the importance of such a moiety to successful encapsulation.

With only two data points, it is unclear whether a tail alone is sufficient to aid the stability of the host-guest complex or whether the nature of the tail is a contributing factor. For example, PBA has a carboxylic acid functional group with eight lone-pair electrons. This observation begs the question of whether potential interactions, such as hydrogen bonding, between the tail and the nanocapsule wall help dock the guest in the supramolecular host. Therefore, investigations focused

on fluorescent probes with lone-pair electron, containing functional groups, particularly pyrene derivatives.

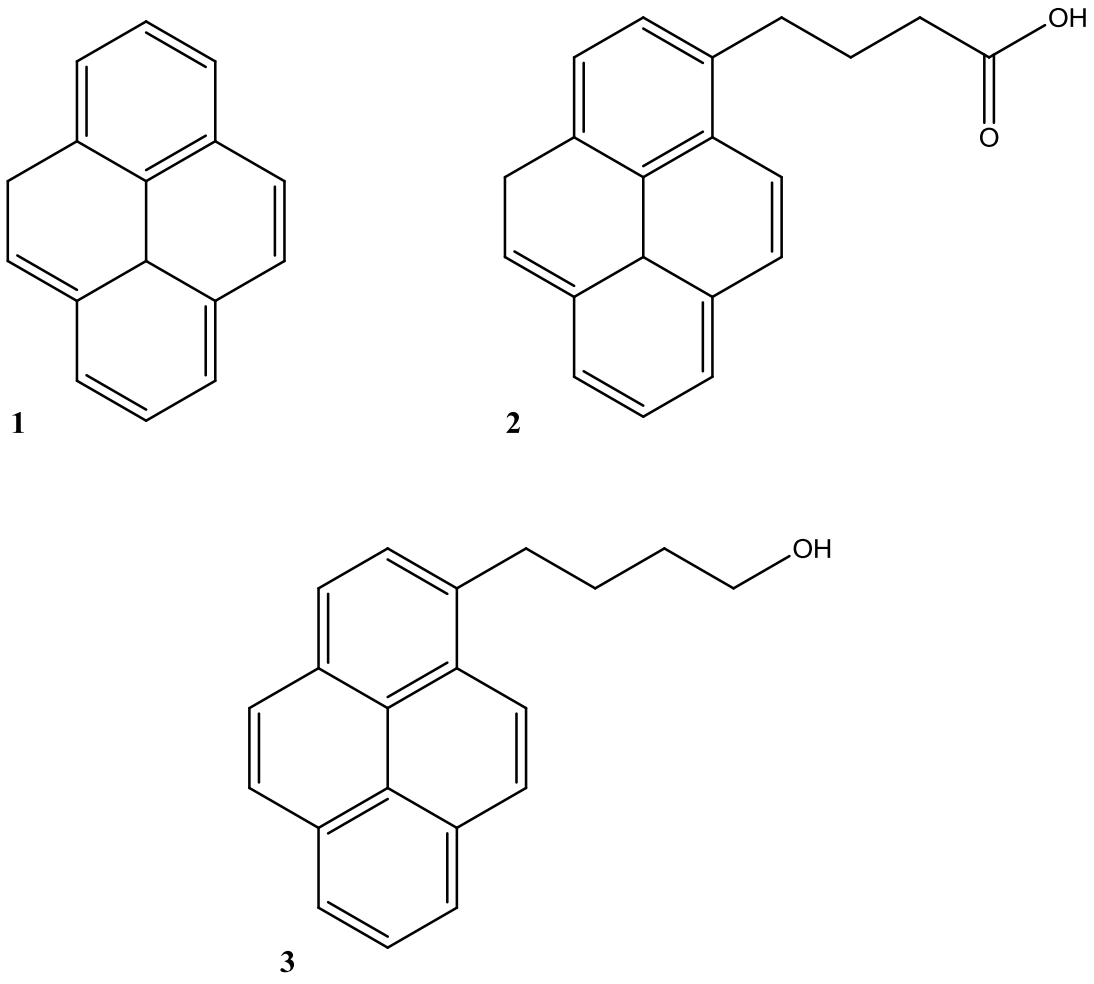

Figure 5.1 Molecular structures of the three pyrene derivatives compared within this work: **1** pyrene, **2** pyrene butyric acid, and **3** pyrene butanol.

Given the success of PBA, pyrene butanol (PyBt, Figure 5.1), was one of the derivatives that appeared to be one of the most promising candidates. Pyrene butanol contains an alcohol functional group with half of the lone-pair electrons as PBA and is a nanoenvironment probe[2-5] with similar molecular and photochemical properties to pyrene and PBA. This unique probe is utilized when differing nanoenvironments are present in the same sample solution. These probes are able to relay information about the specific environment occupied since the probe signal is sensitive to slight changes in the supramolecular assembly. It was hypothesized that the hydroxyl group might introduce additional bonding of the guest with the capsule interior through the functionality of the tail, similar to PBA and unlike pyrene.[2]

II. Results and Discussion:

II.1. Solid State Data:

Capsule-bound PyBt (PyBt-PgC_6) was prepared by the assembly process described in Chapter 3 and is shown schematically in Figure 5.2.

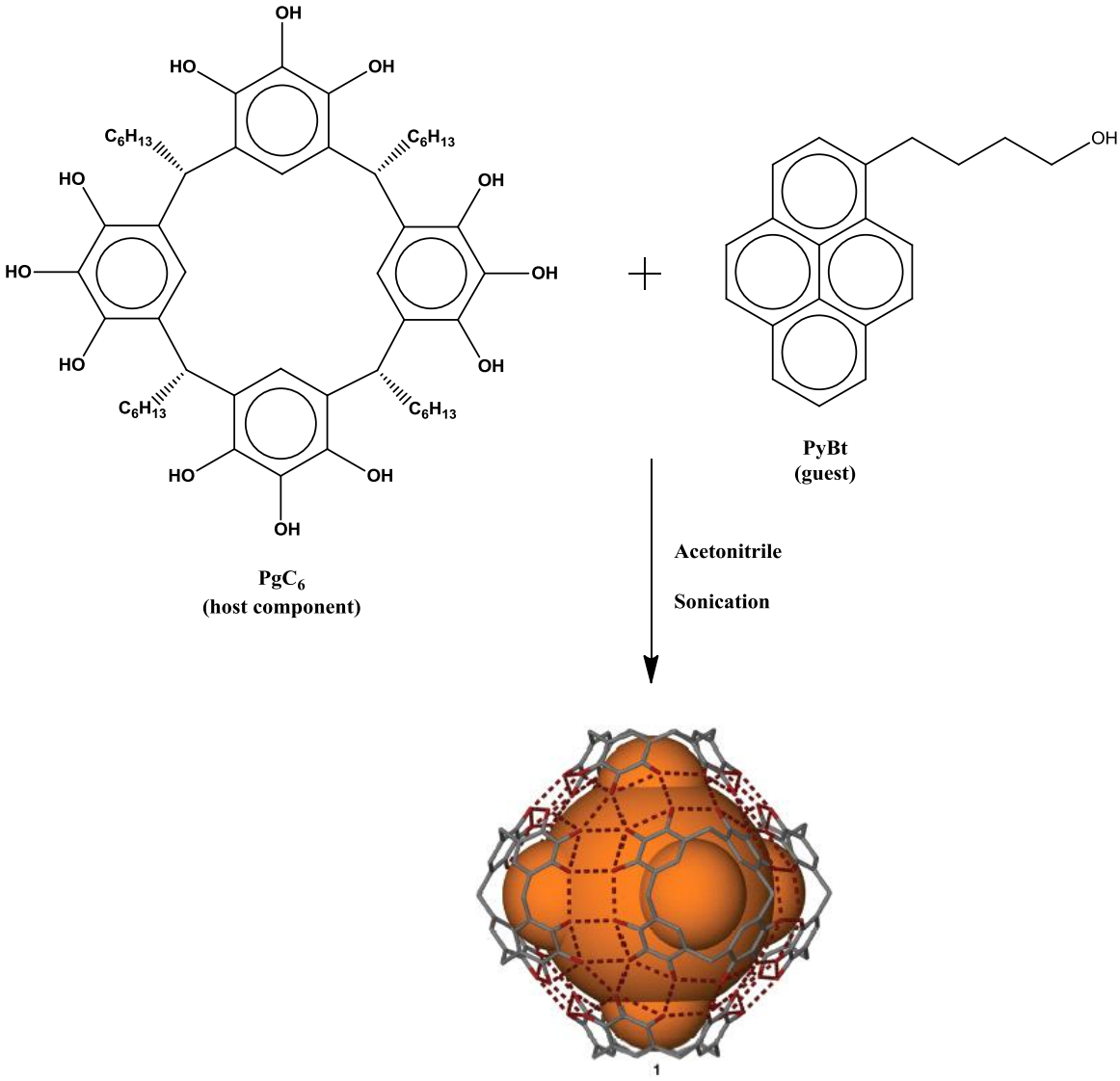

Figure 5.2 Schematic for the formation of hexameric assembly **1** (PgC_6) containing the fluorophore PyBt. The encapsulated space, occupied by PyBt and acetonitrile assemble solvent is depicted in orange.

Pyrene butanol has an approximate volume of 260 Å^3; therefore, sequestering this probe is possible since the interior volume of PgC_6 is ~1250 Å^3.[6]

Single crystal X-ray diffraction studies show that PyBt molecules were ensnared and interact with the nanocapsule walls in the solid state. It was found that up to two PyBt were successfully entrapped within one PgC_6 nanocapsule, and NMR spectroscopy revealed that double occupation occurred in 20% of the population. Previous studies with PBA showed a 50% double occupancy.[2,7] The PyBt molecules are also well separated from one another within the capsule with a pyrene centroid-to-centroid distance of 7.7 Å. This is also similar to previous work done with pyrene butyric acid, PBA.[2] The distance between the π-surfaces of the pyrene substructures of the dye molecules in a doubly occupied capsule is sufficient for one or more acetonitrile (ACN) molecules to occupy. However, it was difficult to determine how many ACN molecules are present due to the diffuse electron density of the system. From the crystal structure (Figure 5.3), it is clear that there is guest-to-wall binding, attributable to π-stacking and CH····π interactions between PyBt and PgC_6. Three crystallographically unique interactions were evident: two CH····π interactions, with CH····aromatic centroid distances similar to

that of the PBA (~2.8 and 2.9 Å); and one π-stacking interaction with an aromatic centroid····centroid distance of 3.87 Å.

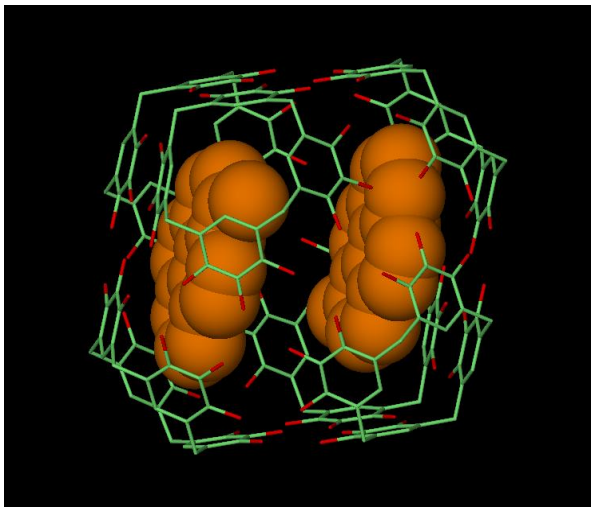

Figure 5.3 X-ray crystallographic structure of encapsulated PyBt in PgC_6, which is represented without the six-chain carbon R-groups.

These results are consistent with the previous work that included PBA.[2] The PBA studies also showed that additional interactions may be present between the tail of the probe and the hydroxyl groups contained in the capsule walls. However, nothing could be definitively proven because of the positioning of the guest, disorder in the system, and the diffuse electron density. The same is also true for PyBt. There is evidence that some interaction could be occurring between the hydroxyl group on the guest 'tail' and the hydroxyl groups contained in the pyrogallol building

blocks that make up the capsule wall, but the same issues that hindered previous confirmation with PBA also hinder the PyBt work: positioning, disorder, symmetry, and electron density. Another aspect that has made this system more difficult to resolve structurally is that the 'tail' of PyBt resides on a plane of symmetry.

II.2 Solution State:

Since many of the supramolecular chemistry applications proposed take place in the solution, it was of interest to find out how these large assemblies react and interact in solution. Molecular spectroscopy was utilized in these investigations.

II.2a Absorption:

The first hint of ground-state interaction in solution is found in the absorption spectrum (Figure 5.4) of encapsulated PyBt in hexane. The absorption spectrum of free PyBt is typical of a pyrene derivative, several well-resolved bands in the UV region. The shifting of the encapsulated PyBt absorbance peaks (~10 nm) as compared to the free PyBt in hexane,

the appearance of a new peak centered around 354 nm, and an overall increase in intensity suggests encapsulation and a ground-state interaction between the probe and the PgC_6 nanocapsule.

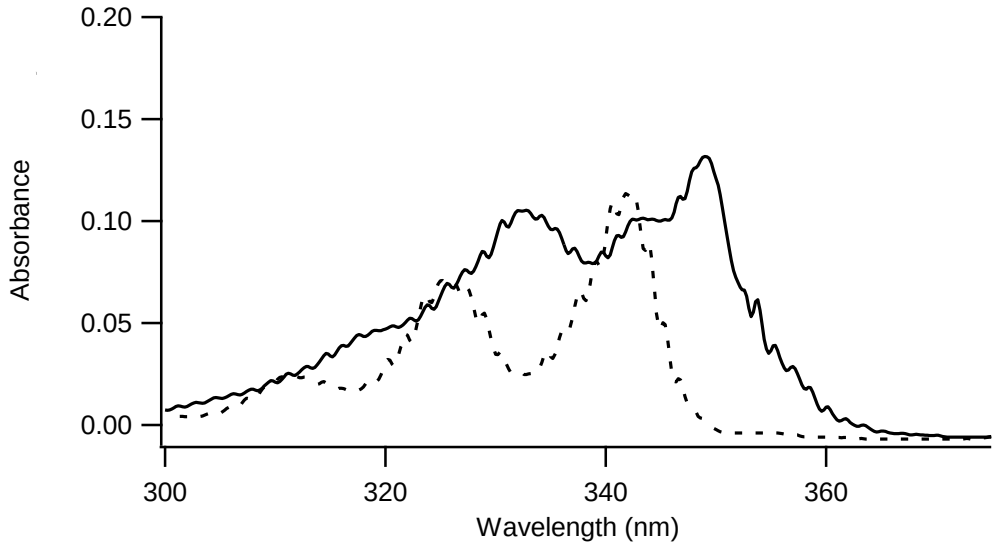

Figure 5.4 Representative absorption spectra of multiple replicates of free PyBt (dotted) and encapsulated PyBt (solid).

This is assumed to be due to the π····π interactions between the aryl groups found in the PgC_6 nanocapsule and the benzene ring of the pyrene moiety. The results from the previous work with PBA were slightly different. There were ground state interactions noted by the appearance of a new peak similar to that seen with PyBt attributable to π-stacking, but the wavelength shift in absorption spectrum was not seen for PBA.

II.2b Fluorescence:

To further examine the host-guest association, the fluorescence emission spectra were collected for both free and encapsulated PyBt (Figure 5.5). At once, the fluorescence emission intensity enhancement (*ca.* four times that of the free probe) for the encapsulated PyBt is noted. This difference is attributable to less collisional deactivation of the excited-state fluorophore, because the capsule provides a protected nanoenvironment for the guests compared to bulk solution.

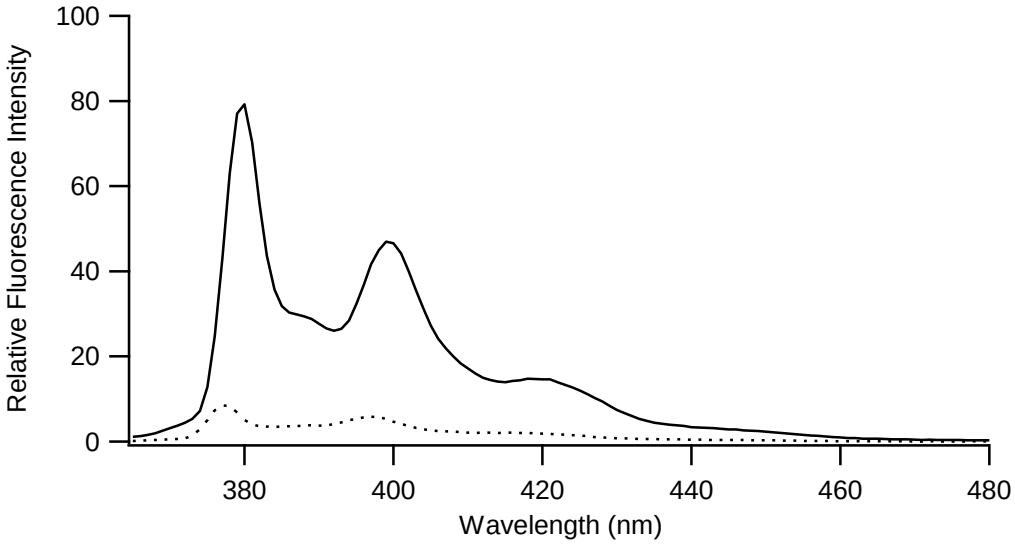

Figure 5.5 Representative fluorescence emission spectra of multiple replicates of free PyBt in hexane (dotted) and encapsulated PyBt in hexane (solid).

This is strong evidence that the probe is still located inside the capsule while in solution at the point in time of the measurement. Another feature to note is the change in intensity of the second band present in the pyrene signature around 390 nm (Figure 5.6 A *versus* B). This small shift is due to excited-state interactions between PyBt and the interior of the capsule, providing further evidence that the probe still is associating with the interior wall of the capsule in solution. Results from encapsulated PBA were similar with a five-fold increase in intensity.

Excimer formation (an excited complex between two monomers) was not observed in either probe assembly. Pyrene derivatives, like PBA and PyBt, exhibit excimer formation in solution. This is readily seen in the emission spectra by the appearance of a broad band at longer wavelengths than the monomer. For example, the monomer emission for pyrene is in the 350-400 nm wavelength region, and the excimer band is at 470 nm.[8] With the absence of an excimer band it can be determined that PyBt molecules, in doubly occupied nanocapsules, are well separated and do not interact with one another. This is also consistent with the solid-state results that showed the spatial separation between the probes in doubly occupied assemblies.

A.

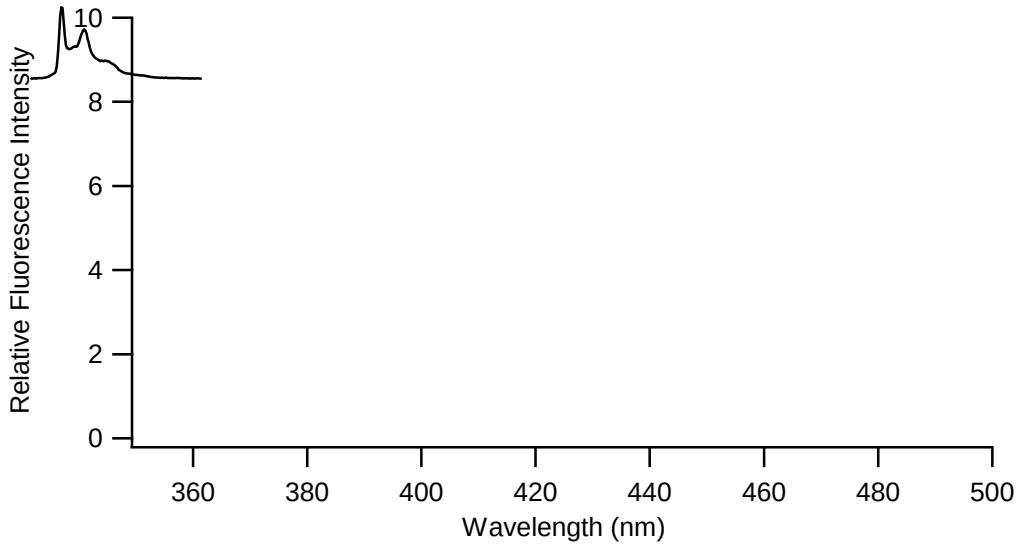

B.

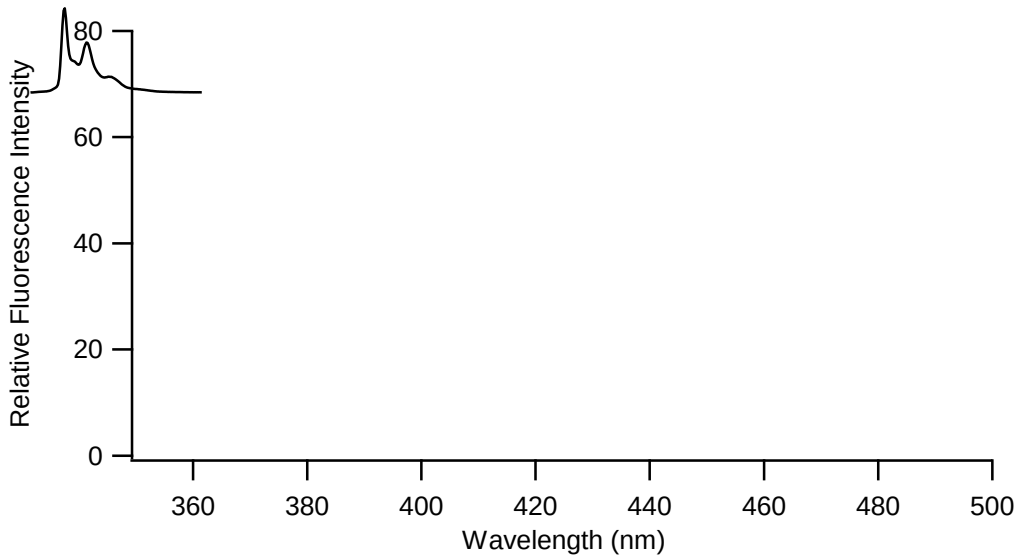

Figure 5.6 Representative fluorescence emission spectra of three replicates of free PyBt (A) and encapsulated PyBt (B) in hexane. Shown on optimized intensity scales to illustrate the evidence of an excited-state interaction at ~390 nm.

Another way to verify that the probe does indeed remain encapsulated even when in solution is by measuring the fluorescence lifetime of PyBt. Table 5.2 shows the average lifetime values (τ in ns) and fractional intensity contributions (α) of free and encapsulated PyBt. The nonlinear least squares analysis of the lifetime data consistently returned just a single, non-noise, lifetime component (τ = 8 or >100 ns) for each sample type. The remarkable lifetime difference, an order of 100 ns, is due to the encapsulation and protection of the PyBt probe. Entrapped molecules have greater emission intensities and longer fluorescent lifetimes due to the protection of the fluorophore from collisional deactivation, which is the primary nonradiative-decay mechanism.

Sample	τ_1 (ns)	α_1	τ_2 (ns)	α_2
Free PyBt	8.5 ± 0.2	1.00	-	-
PgC_6 + PyBt	110 ± 10	0.99	0.00	0.01
Free PBA	8.1 ± 0.2	1.00	-	-
PgC_6 + PBA	120 ± 10	1.00	-	-

Table 5.2 Lifetime data for free and encapsulated PyBt and PBA.

II.2b.1 DMA/ACN:

Once it was confirmed that PyBt remained inside the capsule while in solution, there was a question about the continued presence of assembly solvent molecules, ACN. To test if ACN was present within the capsule as well as the probe, *N,N*-dimethylaniline (DMA) was used. As a fluorescence quencher, DMA is a small molecule that is able to penetrate the hydrogen-bonded seams of the capsule, quench fluorescence, and interact with the PyBt in a predictable manner in the presence of various solvents. In a solution of hexane, DMA will quench the fluorescence of a probe and produce an exciplex (excited-state complex between dissimilar species), represented by a broad, red-shifted emission band. However, in the presence of ACN, the exciplex formation is significantly hindered and wavelength shifted, if detectable at all. Therefore, the presence of ACN solvent molecules can be successfully determined. As mentioned, when DMA is added to a solution of free PyBt in hexane, an exciplex is formed around 445 nm (Figure 5.7).

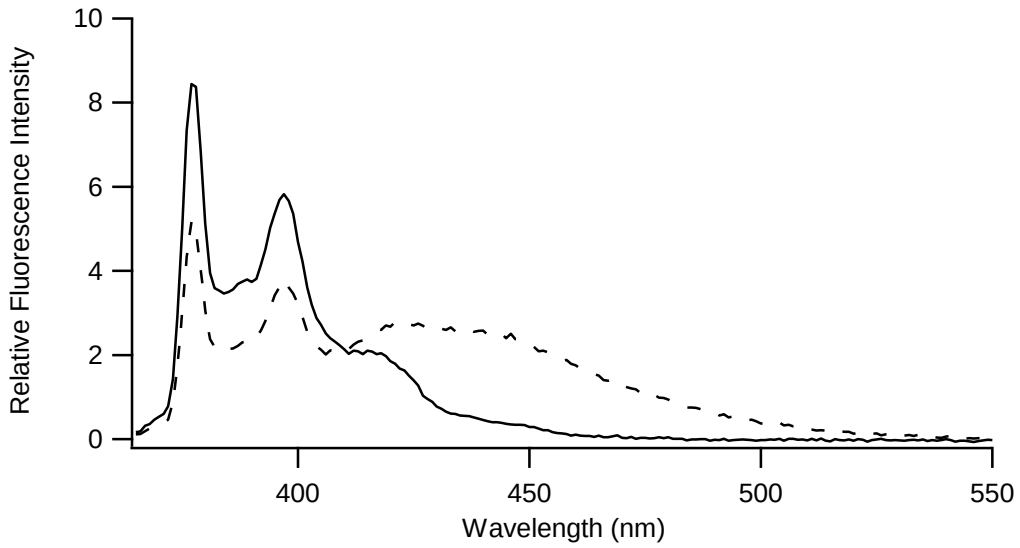

Figure 5.7 Representative fluorescence emission spectra of three replicates of free PyBt in hexane (solid) and free PyBt in hexane with 2 μL of 100% DMA added (dashed).

Upon addition of DMA to the encapsulated PyBt, no exciplex is formed. From Figure 5.8, it is evident that even though the DMA is indeed interacting with the probe, attenuating the fluorescence intensity, there is no evidence of exciplex formation. With no exciplex visibly detected, it can be inferred that ACN molecules must be present to hinder the formation of the exciplex. Pyrene butanol has a molecular volume of 260 $Å^3$ so even with two probe molecules occupying space in the interior of the capsule (1230 $Å^3$) it is still possible for ACN solvent molecules to be present as well. Moreover, they do not appear to diffuse out of the capsule.

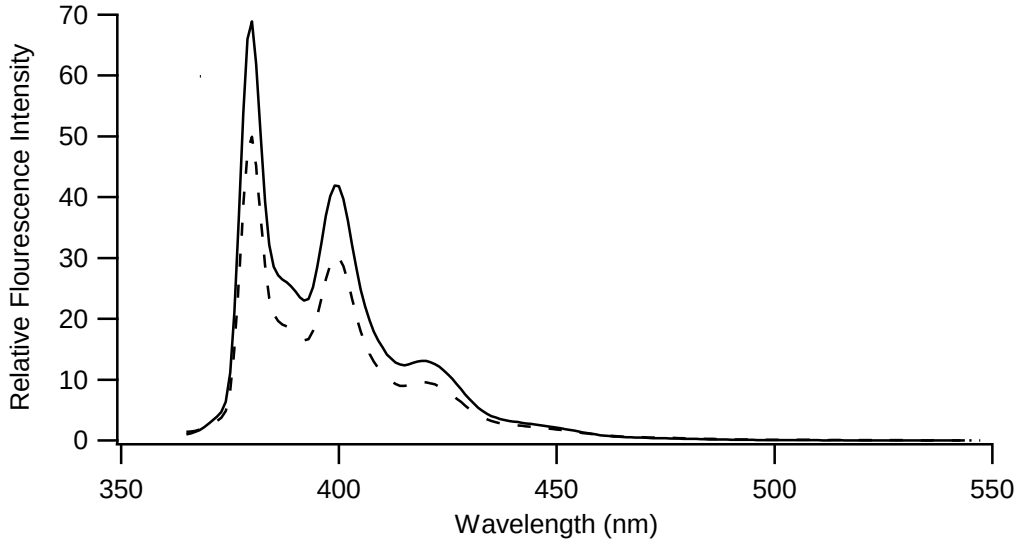

Figure 5.8 Representative fluorescence emission spectra of three replicates of encapsulated PyBt in hexane (solid) and encapsulated PyBt with 2 μL of 100% DMA added (dashed).

Control studies were performed on the previously investigated solutions to verify the absence of exciplex in the presence of ACN. This was done by adding ACN to the solution containing free PyBt and DMA in hexane (Figure 5.9). As clearly seen in the figure below, the exciplex formation is hindered and red shifted when ACN is introduced into the nanocapsule environment. The red shift, from 445 nm to the longer wavelength at 455 nm, for the exciplex emission band correlates with literature.[8]

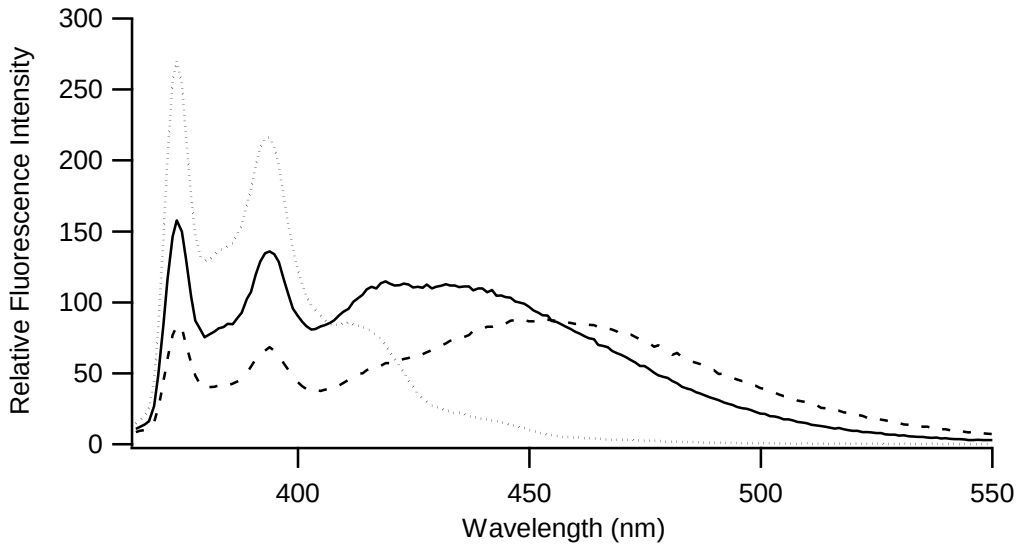

Figure 5.9 Representative fluorescence emission spectra of three replicates of a 2.0 mL sample of free PyBt (dotted), free PyBt with 2µL 100% DMA (solid), and free PyBt with 2µL 100% DMA and 10µL 100% ACN (dashed).

Exciplex formation was not detected when DMA was added to the solution of encapsulated PyBt and ACN (Figure 5.10); therefore, exciplex formation was induced as a control to verify that the presence of the nanocapsule does not alter the quenching mechanism. This was done by the addition of external probe, PyBt, to the aforementioned solution. The hypothesis being since the exo-capsule probe would be in a solution of just hexane, exciplex formation will occur. Once the exciplex has formed, DMA could be added and the interactions monitored.

A.

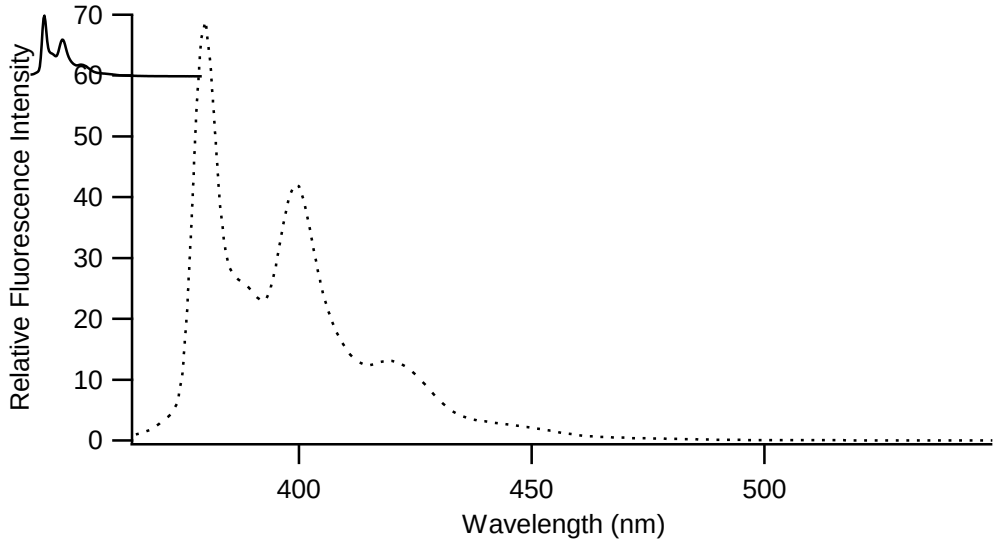

B.

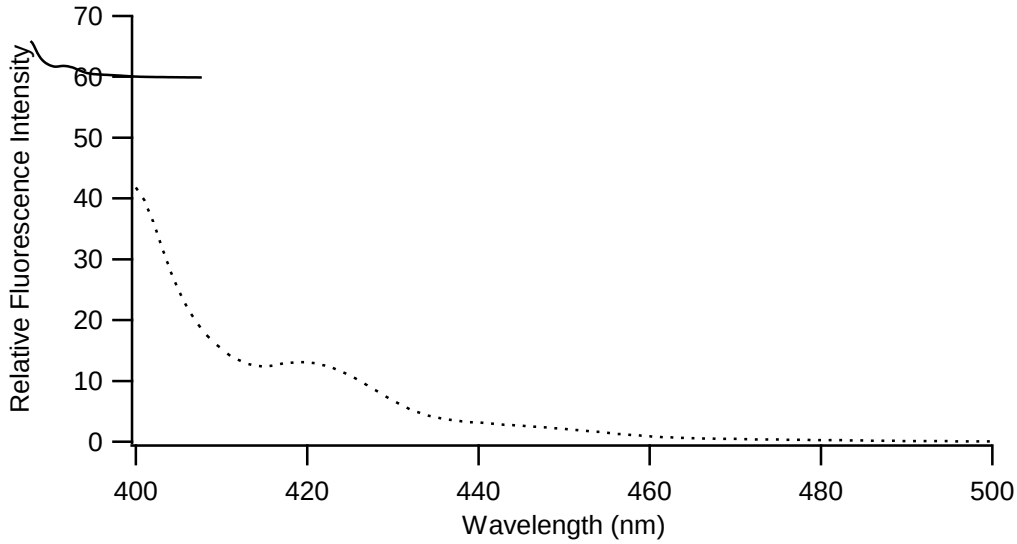

Figure 5.10 Representative fluorescence emission spectra of three replicates of encapsulated PyBt in hexane (dotted) and the same solution with 2µL 100% DMA (solid) is shown in A. B focuses on the exciplex emission wavelength region.

Initially, changes were not observed, which was thought to be a volume or concentration issue. However, once the spectra had been normalized to the 370 nm band, small changes were noted in the 440 – 460 nm spectral region (Figure 5.11).

As seen in Figure 5.11 B, an exciplex does form when exo-capsule PyBt is added to the solution in the presence of DMA. Moreover, when ACN is added to the solution, it quenches the fluorescence intensity, as well as hinders the production of the exciplex. This verified that the results obtained with the encapsulated probe were true results and not due to the interferences caused by the presence of PgC_6 in the solution environment. The previous studies with PBA utilized DMA in the same way discussed above with similar results. The main difference observed was the PBA data did not need to be normalized. The spectral features of the reactions of interest were more readily apparent.

A.

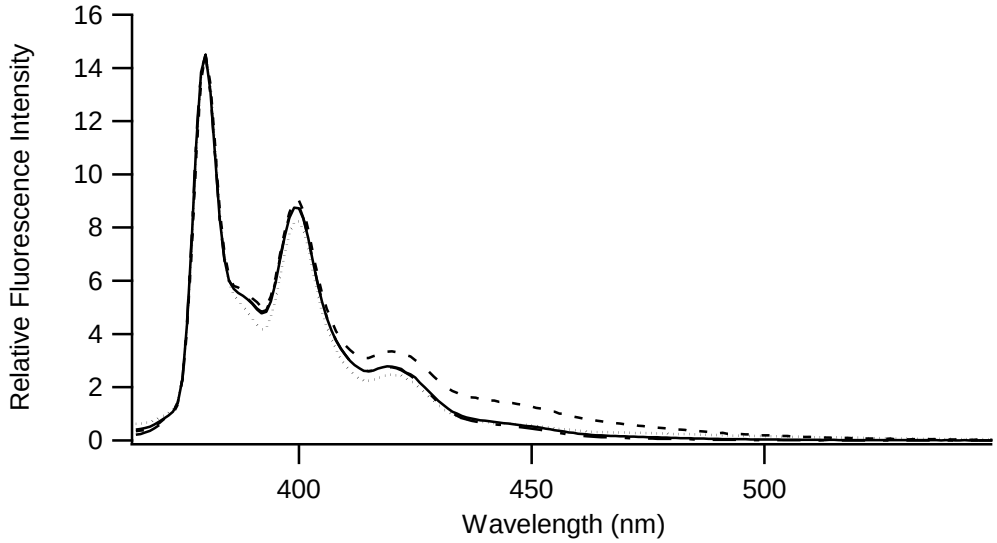

B.

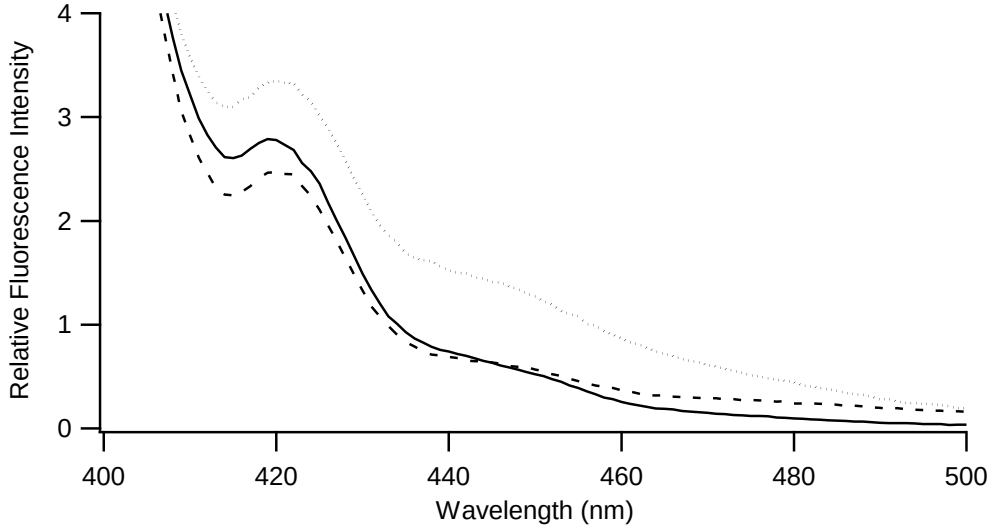

Figure 5.11 Representative fluorescence emission spectra of three replicates of encapsulated PyBt with 2μL 100% DMA (solid), sequential addition of excess exo-capsule PyBt, (10μL) (dotted), and

10μL 100% ACN (dashed) in A. B focuses on the exciplex emission wavelength region.

III. Assembly Stability:

Encapsulating PyBt was fortuitous because it has the exact same structure of what was previously studied, PBA, minus one double-bonded oxygen on the tail, or four lone-pair electrons. So any results from PyBt can be directly compared to PBA and discrepancies could be directly related to 'tail' functionality. This was most evident in the case of assembly stability. The PBA association was found to be structurally robust up to four weeks past encapsulation, with only a 10% loss of probe.[2,7] The PyBt encapsulation was not found to be as robust as PBA. After one week signal strength decreased significantly, and the fluorescence emission signal was no longer detectable under the exact same experimental settings, which were used throughout, after 10 days (Figure 5.12).

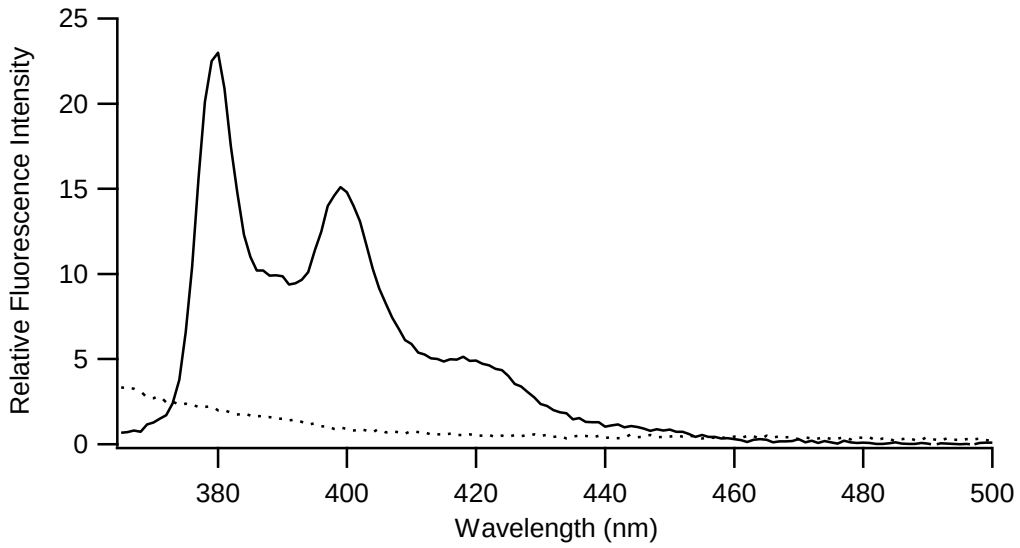

Figure 5.12 Representative fluorescence emission spectra of three replicates of a stock solution of encapsulated PyBt at day 2 (solid) and day 12 (dotted).

IV. Conclusions:

Pyrene butanol was encapsulated in the PgC_6 nanocapsule and studied via solid- and solution-state methods. Up to two PyBt molecules were encapsulated into the host assembly along with ACN solvent molecules. Solution state experiments were utilized to test the ability of the guest to remain encapsulated within the host system. Information obtained on the solvated system included the internal environment and the ability of the complex to act as a nanoreactor for quenching. The DMA quencher was found to be a useful compound in both determining

the presence of ACN within the assembly and illustrating the nanoreactor capabilities.

Results from this PyBt probe were remarkably similar to the previous work with PBA. Both assemblies had the capabilities of entrapping two probe molecules, as well as crystallization solvent, ACN. Double occupation was found to occur 20% of the time for PyBt, which is quite similar to the 50% double occupation of PBA. Both probes were well separated within the assembly by 7.7 Å for PyBt and 7.843 Å for PBA. The main difference observed is in the assembly stability. PBA had a 10% loss in signal intensity after four weeks; whereas, PyBt had almost a 100% loss of signal intensity after a week. This is thought to be due to the 'tail' influence on the host/guest chemistry.

Previous studies have investigated different pyrene derivatives in an attempt to determine the importance of 'tail' functionality in guest encapsulation.[1,7] Results varied depending on functionality and 'tails'. When pyrene was encapsulated in PgC_6, it was unclear if the probe remained within the assembly while in solution. Compared to the pyrene derivatives discussed here, the addition of a linking 'tail' has facilitated better encapsulation.

The size and flexibility of the probe must also be taken into account.[9-10] For example, another probe that was encapsulated in PgC_6 is 1-(9-anthryl)-3-(4-dimethylaniline)propane, ADMA. As seen in Figure 5.12, this probe contains a fluorescent moiety (anthracene) and a quencher (DMA). This allows an intramolecular charge transfer to occur simply by irradiation. The flexibility of ADMA also allows a sandwich-like arrangement, where the two π systems from the anthracene and DMA, stack together.[9-10] This probe showed that conformational flexibility and size can deter the encapsulation process and lead to a higher level of leaching. For example, ADMA contains an anthracene moiety covalently bound by a propyl chain to a DMA molecule. The long carbon chain allows for intramolecular quenching by DMA. The leaching for ADMA in solution was 10% to 44% after 12 days, which was attributed to the probes conformational flexibility.

Other promising results are with *p*-nitro analine and 2,3-diaminonapthalene. The supramolecular assemblies of the respective probes are highly disordered but there is evidence that might indicate encapsulation. All of the results discussed in this body of work have focused on a probe encapsulated in a hexameric spherical assembly. However, this is not the only possible arrangement of these

supramolecular assemblies. Nanotubes and bilayers have been successfully self-assembled with xanthone, aminopyrene, and pyrene.[11] Solid-state fluorescence along with X-ray diffraction are being utilized on these systems presently.

Future studies with guest molecules for this nanocapsule will look into tail length and functionality. Functional groups with lone pair electrons will be tested. Along with the tail, the size and shape of the fluorescent moiety of the probe or PAH will be investigated (length to breath ratio).

V. References:

(1) Bassil, D.B. Ph.D. Dissertation, University of Missouri-Columbia, **2007**.

(2) Dalgarno, S. J.; Tucker, S. A.; Bassil, D. B.; Atwood, J. L. *Science* **2005**,*309*, 2037-2039.

(3) Acree, W. E., Jr.; Tucker, S. A.; Fetzer, J. C. *Poly. Arom. Compd.* **1991**, *2*,75-105.

(4) Hara, K.; Ware, W. R. *Chem. Phys.* **1980**, *51*, 61-68.

(5) Nakajima, A. *Bull. Chem. Soc. Jpn.* **1971**, *44*, 3272-3277.

(6) *The molecular volume of PBA was calculated using Chem3D Ultra 10.0 (www.CambridgeSoft.com)*.

(7) Whetstine, J. L.; Kline, K. K.; Ragan, C. M.; Barnes, C; Atwood, J. L.; Tucker, S. A. *Abstract*, 44th Midwest Regional Meeting of the American Chemical Society, Iowa City, IA, United States, October 21-24 2009.

(8) Lakowicz, J. R. *Principles of Fluorescence Spectroscopy*; Plenum Press: New York, 1983.

(9) Bassil, D. B.; Dalgarno, S. J.; Cave, G. W. V.; Atwood, J. L.; Tucker, S. A. *J. Phys. Chem. B*, **2007**, *111*, 9088-9092.

(10) Dalgarno, S. J.; Bassil, D. B.; Tucker, S. A.; Atwood, J. L. *Angew Chem. Int. Ed.* **2006**, *45*, 1-5.

(11) Dalgarno, S. J.; Cave, G. W. V.; Atwood, J. L. *Angew Chem. Int. Ed.* **2006**, *45*, 570-574.

Chapter 6: Conclusions

The collaboration between the Atwood and Tucker Research Groups continues to generate unique information about the hexylpyrogallol[4]arene (PgC_6) host-guest complexes, leading to a new understanding of their solution-state capabilities. Moreover, this knowledge will allow for the fine-tuning of the nanocapsules to direct the host-guest association. Literature rich in only solid-state studies[1-16] is no longer sufficient for supramolecular chemists. Solution-state studies are becoming more prominent, with this research collaboration's studies at the forefront of the field.[17-19]

The main goal of this research was to investigate the nanocapsule and molecular probe features that enabled encapsulation to occur and remain stable. Highly sensitive analytical techniques, such as molecular spectroscopy, provided information that complements standard single-crystal X-ray crystallographic data. Here new information about how these unique supramolecular assemblies interact with different guests was determined. This collective effort, crossing the solid- and solution-state boundaries, has opened the door on the bountiful information that is useful to the supramolecular community.

A relatively new supramolecular nanocapsule was examined in this work along with a previously investigated capsule. The new nanocapsule contained metal ions (copper) in the place of several of the hydrogen bonds (H-bonds). The $CuPgC_n$ nanocapsule was found to be more structurally stable in the solid state; however, little was known about its solution state chemistry. As expected, compared to the PgC_6 nanocapsule that was seamed together with hydrogen bonds, the $CuPgC_n$ nanocapsule was soluble in a broader range of solvents, excluding that of the extremes (water and *n*-hexane). Fluorescent dyes with many different functional groups, tail lengths, sizes, and shapes were examined for external ligand attachment to or internal encapsulation within the nanocapsule. Exo-capsule attachment of a fluorescent probe was found to be difficult. After multiple attempts and no viable results, an attempt to simplify the system was examined and also unsuccessful.

Internal association or encapsulation was also investigated without much evidence of complexation. The $CuPgC_n$ nanocapsule has the same interior volume as PgC_6. However, after using many fluorescent probes, no crystallographic verification was achieved. Interactions between the fluorescent probes and the nanocapsules were visibly observed due to solution color change, but no solid, either prepicatate or crystal, was

formed. While current work with this specific system is not ongoing, future studies should include other metal-containing supramolecular assemblies that are seamed with metal ions other than copper. This would ensure that issue of potential fluorescence quenching by the metal ion is eliminated as a potential interferent.

In terms of the H-bonded PgC_6 nanocapsules,[17-18] it was hypothesized from previous studies that the functionality of the 'tail' or docking appendage could aid in encapsulation and stability. Moreover, conformational flexibility in the parent moiety was deemed a hindrance to stable complexes. It was thought that the presence of a tail and the availability of specific interactions, such as H-bonding, between the tail and the nanocapsule walls would aid long-term stability. The focus of this research was to test various guests to gain additional understanding of these supramolecular systems. Pyrene derivatives were used to determine if tail functionality of the probe leads to docking stability within the capsule. Pyrene butanol (PyBt), a compound that is structurally similar to the previously studied pyrene butyric acid, was encapsulated within the PgC_6 nanocapsule. Solid-state data revealed that up to two PyBt could be entrapped, PyBt interacted with the interior wall of the capsule, there were 7.7 Å between the two π-systems of the pyrene

modieties, and there were self-assembly solvent molecules, acetonitrile (ACN), present in the interior of the nanocapsule. This directly correlated to solution-state studies, which showed PyBt behaving in the same manner, as found in the solid-state data. When comparing PyBt to the previous studies with PBA, the one main difference found was in solution-state stability. While PBA slowly started leaching out of the PgC_6 nanocapsule over a period of four weeks (10%), PyBt had completely leached from the capsule after little over a week. Comparatively, 1-(9-anthryl)-3-(4-dimethylaniline)propane (ADMA) leached 10% to 44% after 12 days in solution. This adds credence to the hypothesis that the 'tail' group and/or lone-pair electrons aid in stability of the assembly when in solution. Losing one oxygen atom, or two lone-electron pairs, appears to greatly decrease the stability of the encapsulated probe.

Research is still ongoing to determine what parameters are necessary for ideal host-guest association, with long-term solution stability. Some of these parameters might include tail functionality and length (two to six carbon chains), size and flexibility of the fluorescent probe, and functionality contained within the fluorescent moiety. The ultimate goal is to understand the host-guest relationship in such a manner that one can tailor the PgC_6 host-guest association to a given

situation. Work is already on-going that includes probes with other functional groups (e.g., xanthone, *N*-phenyl-1 napthylamine, etc.) and supramolecular assemblies with different R-groups or carbon chain lengths (e.g., PgC_3).

I. References:

(1) Antesberger, J.; Cave, G. W. V.; Ferrarelli, M. C.; Heaven, M. W.; Raston, C. L.; Atwood, J. L. *Chem. Commun.* **2005**, 892-894.

(2) Atwood, J. L.; Barbour, L. J.; Dalgarno, S. J.; Hardie, M. J.; Raston, C. L.;Webb, H. R. *J. Am. Chem. Soc.* **2004**, *126*, 13170-13171.

(3) Atwood, J. L.; Barbour, L. J.; Jerga, A. *Chem. Commun.* **2001**, 2376-2377.

(4) Atwood, J. L.; Barbour, L. J.; Jerga, A. *J. Supramol. Chem.* **2002**, *1*, 131-134.

(5) Atwood, J. L.; Barbour, L. J.; Jerga, A. *PNAS.*, **2002**, *99*,4837-4841.

(6) Atwood, J. L.; Barbour, L. J.; Jerga, A. *Angew. Chem., Int. Ed.* **2004**, *43*,2948-2950.

(7) Cave, G. W. V.; Antesberger, J.; Barbour, L. J.; McKinlay, R. M.; Atwood, J. L. *Angew. Chem. Int. Ed.* **2004**, *43*, 5263-5266.

(8) McKinlay, R. M.; Cave, G. W. V.; Thallapally, P.K.; Atwood, J. L. *Angew. Chem. Int. Ed.* **2005**, *44*, 5733-5736.

(9) Cohen, Y.; Avram, L.; Frish, L. *Angew. Chem., Int. Ed.* **2005**, *44*, 520-554.

(10) Dalgarno, S. J.; Power, N. P.; Antesberger, J.; McKinlay, R. M.; Atwood, J. L. *Chem. Commun.* **2006**, 3803-3805.

(11) Dietrich, B.; Lehn, J. M.; Sauvage, J. P. *Tet. Lett.* **1969**, 2885-2888.

(12) MacGillivray, L. R.; Atwood, J. L. *Nature* **1997**, *389*, 469-472.

(13) Rebek, J., Jr. *Angew. Chem., Int. Ed.* **2005**, *44*, 2068-2078.

(14) Kulikov, O.V.; Rath, N. P.; Zhou, D.; Carasel, I. A.; Gokel, G. W. *New J. Chem.* **2009**, *33,* 1563-1569.

(15) McKinlay, R. M.; Cave, G. W. V.; Atwood, J. L. *PNAS.*, **2005**, *102*, 5944-5948.

(16) Jin, P.; Dalgarno, S. J.; Warren, J. E.; Teat, S. J.; Atwood, J. L. *Chem. Commun.* **2009**, 3348-3350

(17) Dalgarno, S. J.; Bassil, D. B.; Tucker, S. A.; Atwood, J. L. *Angew. Chem., Int. Ed. Engl.* **2006**, *45*, 7019-7022.

(18) Dalgarno, S. J.; Tucker, S. A.; Bassil, D. B.; Atwood, J. L. *Science* **2005**, *309*, 2037-2039.

(19) Whetstine, J. L.; Kline, K. K.; Ragan, C. M.; Barnes, C; Atwood, J. L.; Tucker, S. A. *Abstract*, 44th Midwest Regional Meeting of the American Chemical Society, Iowa City, IA, United States, October 21-24 2009.

VITA

Jena Whetstine was born December 7, 1981 in Columbia, Missouri. She attended Cabool High School in Cabool, Missouri and graduated in 2000. Upon graduation, she attended Truman State University in Kirksville, Missouri and graduated in 2004 with a Bachelor's of Science degree in Chemistry. She attended graduate school at the University of Missouri under the direction of Dr. Sheryl A. Tucker. She was trained as an analytical chemist and completed her Ph.D. in May of 2010.